2021

Nitrogen Dynamics and Transport along Flowpaths in a Rural Wetland-Stream Complex

Colton Kyro

NITROGEN DYNAMICS AND TRANSPORT ALONG FLOWPATHS IN A RURAL WETLAND-STREAM COMPLEX

By

Colton Wilson Kyro

Bachelor of Science, University of Montana, Missoula, Montana, 2018

Thesis

Presented in partial fulfillment of the requirements

for the degree of

Master of Science

in Systems Ecology

The University of Montana

Missoula, MT

August 2021

H. Maurice Valett, Chair

Division of Biological Sciences

Payton Gardner

College of Humanities and Sciences

Matthew Church

Division of Biological Sciences

Kyro, Colton, M.S. Summer 2021 Systems Ecology

Nitrogen Dynamics and Transport along Flowpaths in a Rural Wetland-Stream Complex

Chairperson: H. Maurice Valett

Human activities have doubled the rate of nitrogen inputs onto the landscape resulting in elevated nitrogen concentrations in our streams. Anthropogenically applied nitrogen is largely transported to stream networks via groundwater movement. Groundwater discharge occurs in distinct points along a stream but whose influences can often persist far beyond that area due to insufficient biogeochemical removal of imported nitrogen potentially causing alterations in community structure and precipitating large algae blooms. To understand the factors governing nitrogen abundance in a historical polluted stream, I used a mass-balance approach to quantify groundwater-surface water interaction and the magnitude of groundwater nitrogen input and stream nitrogen removal. I quantified hydrologic and biogeochemical properties of surface and groundwater environments to inform the mass-balance approach and to determine sources of nitrogen to the aquifer. Results identified localized sections of groundwater discharge that were on average 221% of upstream flow. These groundwater inputs were strong controls on the nitrogen budget of the stream and elevated the dissolved inorganic nitrogen concentration and load by 325% and 448% on average, respectively. In-stream nitrification of ammonium-rich groundwater contributed to elevated nitrification rates of 236.21 ± 27.44 mg N m^{-2} d^{-1}. In addition, relatively abundant nitrate concentrations (>0.1 mg N L^{-1}) resulted in high nitrate uptake rates of -358.14 ± 219.78 mg N m^{-2} d^{-1}. An adjacent wetland that covers 1.26 square kilometers was a net sink of nitrogen but had no significant influence on nitrogen transport to the stream due to low substrate permeability. Concentrations of nitrate were correlated to chloride concentrations (r_p=0.80, $p < 0.001$) suggesting the source of groundwater nitrogen originated from municipal effluent that is discharged into the aquifer adjacent to the study reach.

1.0 INTRODUCTION

Humans have doubled the rate of reactive nitrogen (N) inputs into the terrestrial cycle through enhanced atmospheric deposition as well as a variety of land-use practices (Vitousek et al. 1997, Galloway et al. 2004). Inputs of N to the landscape can be transported to aquatic systems via surface hydrologic networks and associated movement of groundwater. In human-altered watersheds, N abundance in aquatic systems is dictated by inputs to the watershed (Howarth et al. 1996, 2011). Specific land-use practices such as agriculture and wastewater disposal have been directly linked to enhanced N loading to recipient river systems (Correll et al. 1992, Turner and Rabalais 2003, Carey and Migliaccio 2009, Hamdhani et al. 2020). Enhanced N loading can have significant influence on streams and rivers because ambient N concentrations in many systems are low and small changes in N loads can dramatically change biotic community structure (Miltner and Rankin 1998, Dodds and Welch 2000), alter function (Mulholland et al. 2008), and cause detrimental ecosystem-wide effects such as algal blooms (Paerl 1997) and eutrophication (Dodds and Smith 2016).

A stream's N abundance can be largely dependent upon internal biogeochemical processing. Low-order streams typically remove reactive N from the channel via biotic assimilation and denitrification (Peterson et al. 2001, Hall and Tank 2003, Mulholland et al. 2009). However, the capacity to mitigate and process N pollution is limited, removal efficiencies decline exponentially with increased N availability as other factors become growth-limiting (i.e., N-saturation, Earl et al. 2006, O'Brien et al. 2007, Mulholland et al. 2008). Nitrogen-saturated systems are characterized by relatively high uptake rates, but reduced uptake efficiency in the face of excess N load, resulting in the propagation of excess N to down-gradient environments (Earl et al. 2006).

Within the stream corridor, chemical composition of water is heavily influenced by exchange flow that link alluvial aquifers to channel waters (Harvey and Gooseff 2015). Groundwater inputs to a given stream reach is dictated by topographic features and hydrogeomorphic gradients, features that may change longitudinally along a stream network (Stanford and Ward 1993, Covino and McGlynn 2007, Jencso et al. 2009) and temporally across seasons (Wroblicky et al. 1998, Jencso and McGlynn 2011). Reach-scale

(0.1-30 km) interactions between surface and sub-surface waters reflect local groundwater systems (*sensu* Toth 1963) that directly interact with streams and differ from intermediate or regional flow paths that integrate larger spatial scales (Winter 1999).

Groundwater discharge can dramatically increase stream flow, import substantial quantities of N, and alter water composition (Covino and McGlynn 2007, Duff et al. 2008, Gilmore et al. 2016). The influence of groundwater on stream water composition, however, is ultimately determined by the interactions between transport and uptake processes that occur along a continuum of biogeochemical environments as water flows through soils and fluvial substrates (McDowell and Likens 1988, Cirmo and McDonnell 1997). Climate and geomorphology dictate the quantity of groundwater transported to a stream (Vogel et al. 1999, Doulatyari et al. 2015) while flowpath character and associated biogeochemical processes determine the abundance of N within it (Cirmo and McDonnell 1997, Tesoriero et al. 2005, Ocampo et al. 2006, Green et al. 2008, Kolbe et al. 2018).

The main process that leads to permanent N removal in groundwater is denitrification (Pinay et al. 1998, Pfeiffer et al. 2006, Baillieux et al. 2014), a respiratory process that reduces nitrate (NO_3^-) to a gaseous form. Rates of denitrification are dictated by the supply of NO_3^-, electron donors, and oxygen (Chappelle 1995, Fabre et al. 2020). Groundwater environments associated with wetland, riparian, and hyporheic zones are often hotspots of denitrification owing to anoxic conditions and an available supply of organic carbon (Vidon and Hill 2004, Ocampo et al. 2006, Pretty et al. 2006, Rivett et al. 2008, Thorslund et al. 2017). Denitrification potential of natural and constructed wetlands in particular have led researchers to advocate for wetland creation to ameliorate N pollution associated with lotic systems (Mitsch et al. 2005, Hey et al. 2012, Cheng et al. 2020).

The efficacy of wetland amelioration of N pollution is dependent upon on its location on the landscape in relation to local flowpaths, which influences the balance between the rate of N transport and N removal. While flow-through wetlands are intimately associated with channel water (Jones et al. 2014), many wetlands are often positioned laterally in relation to stream systems and may be less hydrologically

integrated. Groundwater flowpaths can often avoid wetlands by moving underneath their organic-rich soils and enter streams vertically through the bed (Phillips et al. 1993, Böhlke and Denver 1995, Gu et al. 2008). Regardless of position, transport of N through a wetland is generally dependent upon substrate permeability, a feature that dictates the propensity of porous media to receive and transport water and associated N when exposed to a given hydraulic gradient. Wetlands with low substrate permeability may be supply-limited, reducing the overall mass of N removed (Vidon and Hill 2004); high substrate permeability promotes transport and can limit the efficiency of N removal (Ocampo et al. 2006).

Wetlands may act as sources of N to stream systems reflecting hydrologic alterations (Sapek et al. 2007, Wang et al. 2016) and associated decomposition of deep buried organic material (Sponseller et al. 2018). Dewatering of wetlands increases mineralization of organic material, and accelerates release of stored N (McLatchey and Reddy 1998, Wang et al. 2016). This is especially true for fens, peat forming wetlands that are characterized by dense accumulations of organic material that are normally saturated throughout most of the year. Alterations to their water balances have caused some fens to decompose and mineralize stored N (Sapek et al. 2007, Wang et al. 2016), thereby acting as sources of N to the hydrologic network.

With these associations between wetlands, groundwater, and stream N budgets in mind, I employed a mass-balance approach to determine drivers of N abundance in the Lost Creek-Dutchman Complex (LCDC) in northwestern Montana, USA, a low-order stream-wetland composite potentially influenced by municipal wastewaters. The LCDC is a known source of reactive N to the Upper Clark Fork River (UCFR) and the objectives of the study were to: 1) determine the role groundwater-surface water exchange has on the abundance of N in Lost Creek; and 2) assess the potential for an adjacent fen to influence N loads to Lost Creek. I hypothesized that groundwater-surface water exchange represents a dominant flux in the system's N budget over the course of its flow through the LCDC landscape and that the fen functions as a hotspot of groundwater N loading to Lost Creek due to its landscape position and the influence of seasonal dewatering on net N availability. The LCDC provides an opportunity to address

77 the roles that transport and processing play in both wetland and stream environments and their ultimate
78 influence on nutrient dynamics in the face of enhanced N availability.

79 ## 2.0 METHODS

80 ### 2.1 Study Site

81 The LCDC (46º10'50.4" N 112º50'58.6" W) is a heterogeneous rural stream-wetland landscape that
82 flows into the UCFR near the river's origin (Fig. 1). The complex contains a stream (Lost Creek), a small
83 pond, four spring brooks, and an extensive wetland complex (Dutchman Wetland including the Dutchman
84 Fen). Lost Creek is a low-order stream that drains a watershed of 157 km^2 and has a base flow discharge
85 of ~57 L s^{-1} (USGS 2020). Lost Creek's headwaters reside in a canyon of subalpine mixed coniferous
86 forest. Upon exiting the canyon, Lost Creek flows through a lowland region with upland grasses, willows,
87 and shrubs before entering the LCDC. The LCDC is characterized by a variety of wetland and riparian
88 vegetation including sedges, rushes, mosses, forbs, and woody vegetation that collectively covers ~13
89 km^2 (Applied Ecological Services, 2011).

90 Lost Creek was first identified as a source of inorganic N to the UCFR in 1989 (Ingman and Kerr
91 1990) where it has been found to increase riverine N load at the point of confluence from 2- to 100-fold
92 during the summer months (Hurley and Valett 2019). Treated municipal effluent is released into the
93 aquifer upgradient of the LCDC resulting in elevated groundwater concentrations of NO_3-N and chloride
94 (Cl) reaching up to 10 and 29 mg L^{-1}, respectively (Elizabeth Erickson, Water and Environmental
95 Technologies, pers comm).

96

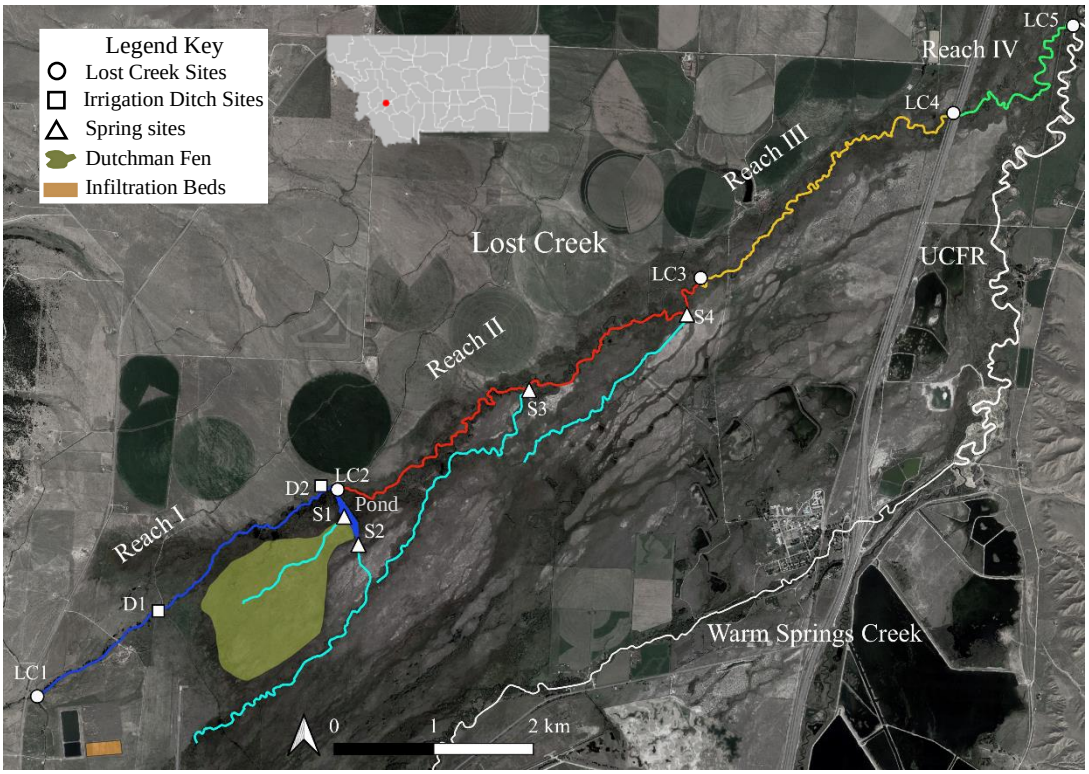

Figure 1: Aerial map of the Lost Creek-Dutchman Complex with Lost Creek, Warm Springs Creek, and the Upper Clark Fork River (UCFR). Lost Creek is delineated into four reaches (I-IV), segmented by five sites on the mainstem of Lost Creek (LC1-5). Two irrigation diversions (D1-D2) remove water from Reach I. Four springs (S1-S4) flow into Lost Creek within reaches I and II. The Dutchman fen and municipal wastewater infiltration beds are adjacent to Reach I. Blue, red, yellow, and green lines depict reaches I-IV of Lost Creek, respectively, whereas light blue lines indicate spring brooks. White lines indicate other lotic water bodies.

97

98 The principal source of groundwater to the system is a surficial unconfined aquifer in unconsolidated
99 valley fills (Konizeski et al. 1968, Fig. S1). The top layer of this aquifer is a large coalescent depositional
100 fan protruding from the mouths of Lost Creek, Warm Springs Creek, and Mill Creek canyons (Konizeski
101 et al. 1968). This layer is 15-30 m deep and consists of interbedded lenses of fine gravel, sand, silt, clay,
102 with carbonaceous soils on the peripheries. Permeability varies within the quaternary alluvium; reported
103 hydraulic conductivities vary from 50-167 m d^{-1} (Water and Environmental Technologies 2003, Barton
104 2018). A deeper secondary layer of approximately 150 m depth includes Pliocene gravel that is poorly
105 indurated and consists of thick-bedded cobble conglomerates intercalated with coarse grained sandstone,
106 tuffaceous siltstone, and thin lenticular shale beds (Wanek and Barclay 1966).

107 I performed mass-balance assessments for the LCDC from May to September 2020 including five and
108 seven sampling occasions for surface and groundwater systems, respectively. The surface water system
109 was divided into four study reaches (I-IV), delineated by five main-channel sites (LC1-5, Fig. 1) while six
110 additional sites were used to track irrigation diversions or groundwater discharge via spring brook input
111 (D1-2, S1-4, Fig. 1). The groundwater system was sampled from a network of piezometers (40) consisting
112 of PVC (200 cm length, 5 cm diameter) installed to an average depth of 100 cm below ground and
113 screened over the final 30 cm, wells (4) installed earlier by Anaconda Deer Lodge County, and stream
114 stage rods (15) located within stream, wetland, and upland environments (Fig. 2a).

115 **2.2 Sampling**

116 Surface and groundwater systems were sampled within the same week on a monthly basis from late
117 May to early October. I measured physiochemical conditions, hydrologic discharge, and sampled water
118 for dissolved nutrient concentrations from surface water sites (Fig. 1). I measured the hydraulic head from
119 each piezometer and stream stage rod, and used water table measurements from four wells (Fig. 2a)
120 monitored by Anaconda Deer Lodge County and Montana Bureau of Mines and Geology when sampling
121 dates corresponded (Elizabeth Erickson, Water and Environmental Technologies, pers comm, MBMG
122 2021).

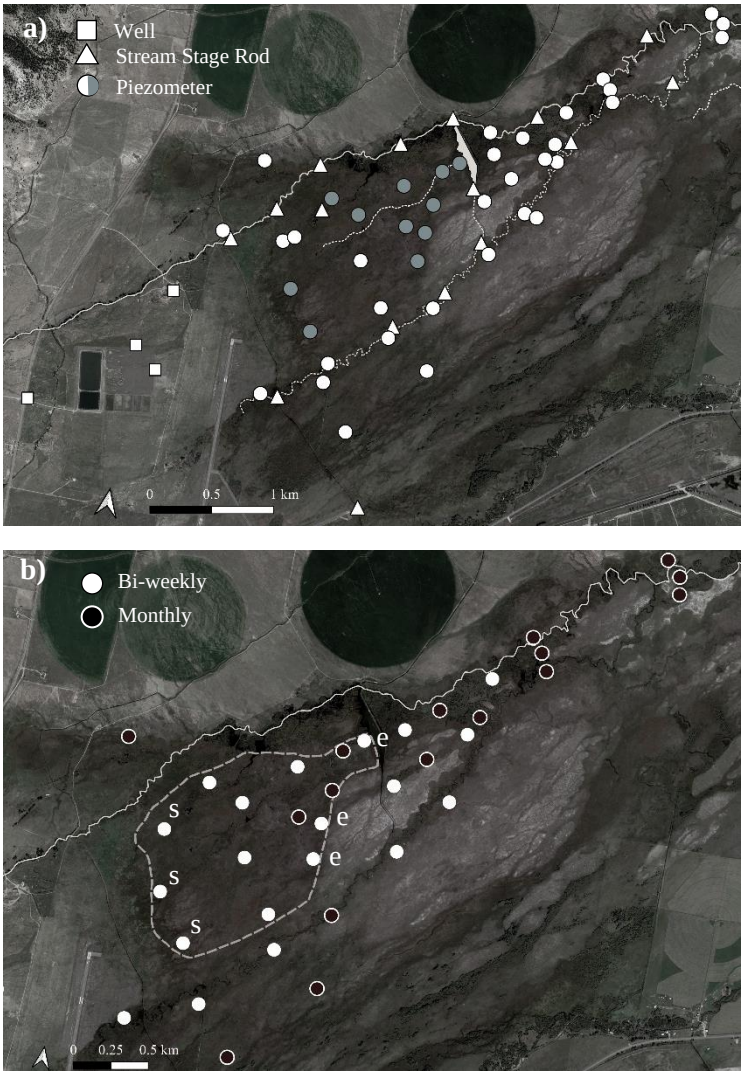

Figure 2: Aerial map of the Lost Creek-Dutchman Complex and associated sampling locations. Grey lines and polygon denote Lost Creek and its pond. Grey dotted lines and dashed lines indicate spring brooks and the fen's approximate boundaries, respectively. a) Circles indicate piezometers (40) installed for hydrometric and water quality data acquisition. Grey circles indicate piezometers used to assess hydraulic conductivity. White triangles indicate stream stage rods (15) and white squares indicate wells (4) monitored by Anaconda Deer Lodge County and Montana Bureau of Mines and Geology. b) White circles are piezometers (20) sampled bi-weekly and black circles indicate piezometers (16) sampled monthly. The dashed line depicts approximate fen boundaries. Piezometers with an adjacent "s" or "e" indicate those used to address start and end of fen flowpaths, respectively (see text for explanation).

123

In addition, I measured physiochemical conditions and sampled groundwater for dissolved nutrient concentrations from the piezometer network (Fig. 2b) on a bi-weekly basis from 20 piezometers and monthly from 16 others (Fig. 2b).

Physiochemical measurements, measured by YSI probes (YSI Inc./Xylem Inc., Rye Brook, NY), included specific electrical conductivity (µS cm^{-1}), dissolved oxygen (mg L^{-1}), pH, and temperature (°C). Stream flow (Q, L s^{-1}) was collected from a USGS gaging station (#12323850 at site LC4) and via a handheld acoustic Doppler velocimeter (Xylem Inc., Rye Brook, NY) employing the area-velocity approach (ISO 2007). I measured the hydraulic head of my piezometers and stream stage rods using a Mini Water Level Meter (Solinst Canada Ltd, ± 2.0 cm). Piezometer and stream stage rod elevations were determined by a LiDAR digital elevation model (Tom Parker, Geum Inc., unpublished data).

Water samples were collected in triplicate either from the thalweg of the stream or from piezometers using a Geopump peristaltic pump (Geotech Environmental Equipment, Inc. Denver, CO). Piezometers were purged and allowed to refill before sampling occurred. Water samples for dissolved nutrients were filtered through a glass-fiber filter (0.7 µm pore size, Whatman PLC, Boston, MA), stored on ice, and transported to the lab where samples for NO_3-N (mg L^{-1}), ammonium-N (NH_4-N; mg L^{-1}), soluble reactive phosphorus (SRP; mg L^{-1}), and Cl (mg L^{-1}) were frozen (-20°C) and samples for dissolved organic carbon (DOC; mg L^{-1}) refrigerated (3.5°C) until further analysis. I analyzed samples of NO_3-N, NH_4-N, SRP, and Cl using a Flow Injection Analyzer (FIA, Astoria-Pacific, OR). Concentrations of NH_4-N were determined using the phenol-hypochlorite method (USEPA 1993a). Concentrations of NO_3^- + nitrite were assessed using the cadmium-reduction method (USEPA 1993b) and reported here as NO_3-N. Dissolved inorganic N (DIN) was determined by summing the concentrations of NH_4-N and NO_3-N for each sample. Concentrations of SRP were assessed using the ascorbic acid method (USEPA 1993c) and Cl concentrations determined using the ferricyanide colorimetry method (U.S. EPA 1986). I measured DOC concentrations using an Aurora 1030W Total Organic Carbon (Xylem Inc., Rye Brook, NY) employing the heated persulfate oxidation method (U.S. EPA 2005).

149 **2.3 LCDC Hydrology**

150 I used a mass-balance approach, along with geospatial analysis, to determine the magnitude of stream
151 flow into and out of designated reaches, groundwater exchange with Lost Creek, and direction of
152 groundwater movement within the adjoining wetland complex. Without accounting for
153 evapotranspiration, net groundwater exchange (Q_{gw}, L^3T^{-1}) was calculated as the change in discharge
154 between upstream and downstream reach boundaries once corrected for channelized losses using:

155 $$Q_{gw} = Q_d + Q_{ir} - Q_u \quad (1)$$

156 where Q_{gw} is determined as the difference between reach losses via downstream discharge (Q_d) and
157 irrigation diversion (Q_{ir}) and water inputs from upstream (Q_u). Positive Q_{gw} values represent groundwater
158 discharge into the stream whereas negative values represent net hydrologic losses to groundwater.
159 Irrigation diversions in Reach III were intermittently flowing, were not gauged, and represent a source of
160 error for mass-balance in that reach.

161 Net groundwater exchange was further differentiated by specific groundwater discharge pathways
162 including diffuse groundwater and spring brook:

163 $$Q_{gw} = Q_{dif} + Q_{spr} \quad (2)$$

164 where Q_{dif} is groundwater discharge from diffuse groundwater input and Q_{spr} is groundwater discharge
165 from spring brooks.

166 Hydraulic head measurements from piezometers, stream stage rods, and wells were used to develop a
167 variogram in R (R Core Team 2020 V 4.0.3) that interpolates values between spatially discrete sites of
168 measurement using ordinary kriging (gstat, Pebesma 2004, Gräler et al. 2016). Hydraulic head
169 measurements, assumed to be the elevation of the water table, were used to create a variogram that
170 determined the weighted average to inform the kriging that generated a raster representation of elevation

171 across the piezometer network. Water table rasters were contoured to produce equipotential lines used to
172 produce flow nets showing the direction of groundwater movement.

173 **2.4 Lost Creek N Budget**

174 I performed mass-balance assessments to address changes in nutrient abundance using material loads
175 (i.e., L) derived as product of Q and concentration (Burns et al. 1998a, Brown et al. 2007, Gilmore et al.
176 2016). Change in load (ΔL, MT^{-1}) was calculated for each of the four delineated reaches on five sampling
177 dates between late May and early October. Mass-balance of solute loads (ΔL) for each reach was
178 calculated as difference between outputs and inputs:

179 $$\Delta L = L_d + L_{ir} - L_u \quad (3)$$

180 where L_d is downstream solute load, L_{ir} is solute load lost to irrigation diversion, and L_u is the upstream
181 solute load. Change in load (ΔL), represents net alteration and includes all in-stream biogeochemical
182 processes occurring along the reach as well as net loading due to groundwater exchange.

183 Change in load was further parsed by delineating the putative influences of groundwater exchange
184 and biogeochemical processing:

185 $$\Delta L_{bio} = \Delta L - \Delta L_{gw} \quad (4)$$

186 $$\Delta L_{gw} = Q_{dif} * C_{dif} + L_{spr} \quad (5)$$

187 where ΔL_{bio} is the estimated change in solute load due to biogeochemical processing, ΔL_{gw} is the
188 estimated change in solute load due to exchange with groundwater, L_{spr} is the load entering a reach from
189 spring brooks, and C_{dif} is the average concentration of a solute from water entering or leaving the channel
190 depending on whether the reach is losing or gaining during the sampled period. During the first sampling
191 date (May 31st), spring brooks S1, S3, and S4 were not gauged and values from the nearest time under
192 similar flow conditions were used as representative values for that sampling. When change in discharge
193 over the length of the reach indicated net groundwater recharge (i.e., $Q_{dif} < 0$), the geometric mean of

surface water concentrations for a given solute was used to represent C_{dif}; groundwater concentrations were used when net diffuse groundwater input occurred ($Q_{dif} > 0$). Average groundwater concentration was calculated as a weighted mean. We used the average hydraulic conductivity of the substrate each piezometer was in to weight the samples for chemical composition following Chestnut and McDowell (2000).

To assess how well subsurface monitoring values represented the potential composition of actual aquifer discharge to Lost Creek, I compared the concentrations of a conservative ion (Cl) derived from my piezometer network as described with the calculated values for diffuse groundwater inputs generated through mass-balance. The calculated Cl concentrations for diffuse groundwater inputs were derived as mass-balance residuals following Gilmore et al. (2016):

$$Cl_{dif} = \frac{L_{d\,Cl} - L_{u\,Cl} - L_{s\,Cl}}{Q_d - Q_u - Q_s} \quad (6)$$

where Cl_{dif} is the concentration of Cl in diffuse groundwater input for a given stream reach and $L_{d\,Cl}$, $L_{u\,Cl}$, and $L_{s\,Cl}$ are the loads of Cl from downstream, upstream, and spring brooks, respectively. I calculated Cl_{dif} on every sampling date for reaches that had diffuse groundwater input and compared those values to the estimated Cl concentration derived from the weighted average.

Reach specific ΔL, ΔL_{bio}, and ΔL_{gw} were separately summed within each sampling date to derive whole-system measures of load change for Lost Creek (ΔL_{LC}) for a given N species that can be attributed to groundwater exchange (ΔL_{GW}) and biogeochemical processing (ΔL_{BIO}). I normalized ΔL_{bio} to bed area to generate effective biogeochemical fluxes (U_{bio} $ML^{-2}T^{-1}$) that can be compared among the four reaches and with other aquatic ecosystems using:

$$U_{bio} = \Delta L_{bio}/(w * L) \quad (7)$$

where w is the average wetted width of the reach, L is the length of the stream reach, and U is the effective solute flux. Positive U_{bio} values represent solute production whereas negative values represent solute removal.

2.5 Fen Characterization and N Processing

I characterized the fen's spatial dimensions, hydrologic properties, and the chemical composition of its pore water to address its functioning at the landscape level. The areal extent of the fen (L^2) was determined by tracking its exterior, delineated by the transition between wetland and grassland vegetation, using a GPS eTrex® 20x unit (Garmin Ltd., Olathe, Kansas) and mapping the points on ArcGIS (ESRI 2020). Depth of fen material was measured by inserting a steel probe into the fen until it met resistance from underlying mineral substrate. Depth to resistance (L) was recorded as the thickness of the fen. I determined the hydraulic conductivity of the fen by performing slug tests (Bouwer and Rice 1979, Bouwer 1989) on 12 piezometers (Fig. 2b) within its boundaries using a pressure transducer (kPa, Onset HOBO U20L, Bourne, MA) to track changes in hydraulic head.

I subtracted each monthly water table raster from the first (i.e., May 2020, when water table elevation was greatest) using QGIS (QGIS 2020 V 3.12.0) to show cumulative changes in groundwater depth during the growing season within the fen. I also quantified the volume (L^3) of the fen drained sequentially during the course of the season by subtracting the LiDAR digital elevation model of the fen (clipped to the area of the fen) from each monthly water table raster using QGIS (QGIS 2020 V 3.12.0) to represent the average depth to the water table within the fen. The average depth to the water table was multiplied by the areal extent of the fen to derive a volume of unsaturated media for each month.

A mass-balance approach was used to quantify changes in the loads of specific solutes (NO_3^-, NH_4^+, DIN) as groundwater entered and left the fen following approaches used by Clément et al. (2003), Vidon and Hill (2004), and Zhang et al. (2009). Groundwater inputs and outputs within the fen were estimated by creating theoretical flowpaths guided by flownets (Casagrande 1937, Bennet 1962) generated from

239 water table mapping. I generated streamlines guided by equipotential contours to produce three flowtubes
240 that encompass the majority of the fen. Flowtubes were placed to ensure that each included a monitoring
241 piezometer at the start and end of its length. For each flowtube, I calculated the longitudinal movement of
242 groundwater (L^3T^{-1}) through a given cross-section using Darcy's law:

243 $$Q = -K * w * z * \frac{dh}{dl} \quad (8)$$

244 where Q is volumetric movement of water, K is average hydraulic conductivity of the fen, w is average
245 width of the flowtube, z is average saturated depth of the flowtube, and $\frac{dh}{dl}$ is the hydraulic gradient (i.e.,
246 change in head over tube length). Flowtube width, length, and change in hydraulic head were determined
247 from the fen's spatial extent, flownet data, water table rasters, and length measuring tools in QGIS (QGIS
248 2020 V 3.12.0). The saturated depth of flowtubes was estimated from the depth of the water table and fen
249 material within each flowtube.

250 I estimated the production or removal of a solute (MT^{-1}) as water moves through a given flowtube
251 using:

252 $$\Delta L_i = Q_i * \left(C_{i\,(end)} - C_{i\,(start)} \right) \quad (9)$$

253 where for each flow tube 'i', ΔL_i is change in solute load, Q_i is the volumetric movement of water moving
254 within the tube, and $C_{i\,(end)}$ is the concentration of a solute at the end and $C_{i\,(start)}$ the concentration at the
255 beginning of a tube. The concentration of a solute entering and leaving a flowtube was determined from
256 piezometers on the up-gradient and down-gradient edges of the fen associated with each flow tube (Fig.
257 2b). I calculated the fen's overall influence on groundwater N transport (ΔL_F) by summing the changes in
258 DIN load from each flowtube within each sampling date.

259 **2.6 Data Analysis**

260 I used a Kruskal-Wallis rank sum test and a non-parametric multiple comparison test (Siegel and
261 Castellan 1988, $p < 0.05$) using the R package pgirmess (Giraudoux 2021) to compare behavior among

reaches. In addition, one-sample t-tests for location were used to determine if mean measures of reach function were different than zero. A paired t-test was used to determine if Cl concentrations derived from the piezometer network were different from those calculated for diffuse groundwater using Eq 6. Pearson correlation coefficient was used to determine the correspondence between N and Cl concentrations. All statistical analysis were performed in R (R Core Team 2020 V 4.0.3).

3.0 Results

3.1 Background Chemistry

Lost Creek and its surrounding groundwater differed markedly in physiochemical character (Table 1). Lost Creek was well oxygenated with high dissolved oxygen concentrations (10.18 ± 0.25 mg L^{-1}, grand mean ± standard error), whereas groundwater was generally hypoxic (1.49 ± 0.12 mg L^{-1}) with 66% of DO measurements less than 1 ppm. Temperature of both Lost Creek and groundwater increased throughout the sampling season but to different extents. Lost Creek averaged 12.9 ± 0.5°C and varied from 4.8 to 22.5°C. Whereas groundwater was cooler and less temporally variable, with temperatures ranging from 6 to 16.3°C with an average value of 10.13 ± 0.1°C. The pH of water within the LCDC was basic with values of 8.48 ± 0.05 and 7.73 ± 0.05 for Lost Creek and groundwater, respectively.

In tandem with physiochemical differences, nutrient concentrations in surface water and groundwater differed within the LCDC (Table 1). Although Lost Creek and groundwater had similar concentrations of DIN (0.209 ± 0.022 and 0.218 ± 0.024 mg L^{-1}, respectively), they displayed contrasting trends in regards to concentrations of specific inorganic N species. Nitrate was 95% of DIN in Lost Creek but only 27% within groundwater where DIN was primarily NH_4-N. Groundwater concentrations of DOC were distinctly greater and exhibited more extensive variability than seen for Lost Creek. Groundwater DOC concentrations ranged from 0.327 to 40.199 mg L^{-1} with an average of 6.673 ± 0.466 mg L^{-1}, whereas Lost Creek's DOC concentrations ranged from 0.725 to 4.217 mg L^{-1} and had an average of 2.282 ± 0.198 mg L^{-1}.

286 The average hydraulic conductivity-weighted concentrations of groundwater NH_4-N, NO_3-N, DIN
287 and Cl were 0.186, 0.105, 0.286, and 9.179 mg L^{-1}, respectively. The average flow-weighted Cl
288 concentration of diffuse groundwater input was 8.141 ± 1.172 mg L^{-1} (Table S1), which was not different
289 ($p > 0.05$) from the average hydraulic conductivity-weighted Cl concentration of groundwater.

290 **3.2 Lost Creek Hydrology and Groundwater Movement**

291 Flow in Lost Creek was altered by seasonality, irrigation withdrawals, and groundwater discharge.
292 Flow in Lost Creek generally declined with snowmelt recession into baseflow (Fig. S2a). Irrigation
293 withdrawal during May and July resulted in Reach I losing water over its length even though the reach
294 experienced consistent net groundwater input (Fig. 3). During later sampling dates, stream flow increased
295 within Reach I, while flow within Reach II increased during all sampling dates (Fig. S2a) as a result of
296 persistent groundwater inputs (Fig. 3) and lack of irrigation withdrawal. Flow generally declined within
297 reaches III and IV reflecting surface water infiltration into the groundwater systems (i.e., negative net
298 groundwater exchange, Fig. 3) and intermittent irrigation withdrawals that were not measured.

299

300

301

Table 1: Summary statistics of various physiochemical conditions and nutrient concentrations from Lost Creek and nearby groundwater monitoring sites.

Statistic	Dissolved Oxygen (mg L^{-1})	Temperature (°C)	pH	Specific Conductivity (µs s^{-1})	NH_4-N (mg L^{-1})	NO_3-N (mg L^{-1})	DIN (mg L^{-1})	Cl (mg L^{-1})	SRP (mg L^{-1})	DOC (mg L^{-1})
Lost Creek										
Grand Mean	10.42	13.44	8.48	431.9	0.010	0.199	0.209	4.420	0.006	2.282
Standard Error	0.30	0.72	0.05	38.4	0.002	0.021	0.022	0.387	0.001	0.198
n	25	25	25	25	25	25	25	25	24	25
Median	10.12	13.60	8.46	421.5	0.007	0.216	0.241	4.792	0.007	2.332
Min	7.99	6.90	7.89	120.1	0.001	0.018	0.025	0.845	0.001	0.725
Max	13.29	19.10	9.07	1135.2	0.052	0.415	0.416	7.124	0.015	4.217
Groundwater										
Grand Mean	1.44	10.13	7.73	710.6	0.159	0.060	0.218	10.178	0.015	6.673
Standard Error	0.12	0.12	0.05	25.9	0.020	0.016	0.024	0.481	0.001	0.466
n	222	247	38	172	196	197	197	197	185	176
Median	0.76	10.0	7.71	647.0	0.066	0.004	0.083	7.927	0.008	5.356
Min	0.03	6.0	7.22	3.5	0.003	0.001	0.003	2.126	0.001	0.327
Max	8.47	16.3	8.63	2543.0	1.619	1.352	1.628	36.334	0.150	40.199

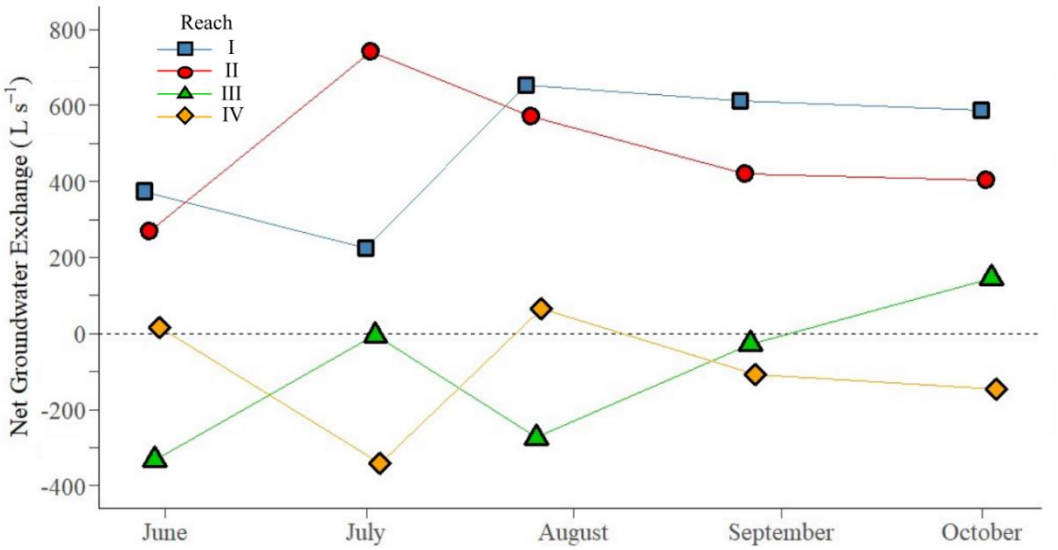

Figure 3: Net groundwater exchange (L s^{-1}) along Lost Creek's four reaches on each sampling date. Positive net groundwater exchange values indicate groundwater inputs into the reach whereas negative values indicate surface water infiltrating into the groundwater system. Data are single measures derived from hydrologic mass balance.

315 Water inputs from spring brooks were fairly consistent compared to channel flow. Flow from the
316 largest spring brook in the system (S2) averaged 295 ± 9 L s^{-1} (mean ± standard error) and differed by
317 only 16% across all sampling dates. Flows in spring brooks S1, S3, and S4 showed greater seasonality,
318 on average declining 68% from July to September until increasing again in October (Fig. S2b). Irrigation
319 diversion withdrawals varied but generally declined from spring to late summer (Fig. S2b).

320 As a percentage of upstream inputs, total groundwater discharge into Lost Creek varied from 44-
321 515%, averaging 221%. Smaller percentages occurred during snowmelt when stream flows were greater
322 entering study reaches, whereas inputs from groundwater were proportionally larger following snowmelt
323 when channel flow was reduced. Groundwater inputs were associated with both spring brooks and diffuse
324 groundwater. Average flow was greater for spring brooks than for diffuse groundwater inputs in Reach I
325 (Fig. S3a). In contrast, diffuse groundwater inputs to Reach II were nearly double the flow contributed
326 from spring brooks (Fig. S3b).

327 Direction of groundwater movement was fairly stable during the growing season, especially within
328 the wetland areas including the fen (Fig. S4). Across sampling dates, flow lines were generally parallel to
329 the stream channel, but fluctuations in groundwater flowpath direction occurred within the upland area
330 near the infiltration beds during periods of high flow (late May to early July, Fig. S4a-b). Flow direction
331 then stabilized through the remainder of the growing season (Fig. S4c).

332 **3.3 Spatiotemporal Patterns in Surface Water N Concentration and Load**

333 Lost Creek exhibited both longitudinal and temporal variation in N concentration. Throughout the
334 growing season and under various flow regimes, DIN and NO_3-N concentrations increased in reaches I
335 and II and then declined in reaches III and IV (Fig. 4a-b). On average, DIN concentrations increased by
336 325% over the length of Lost Creek. Trends in DIN reflected alterations in NO_3-N as concentrations of
337 NH_4-N were low and showed little consistent longitudinal or temporal trends (Fig. 4b). Changes in DIN
338 concentrations were most striking in Reach I, exhibiting both longitudinal and temporal variability. In

early July, DIN concentrations increased 500% from 0.026 ± 0.001 to 0.156 ± 0.005 mg L^{-1} (mean ± standard error) over the length of Reach I while a month later they rose from 0.039 ± 0.008 to 0.417 ± 0.009 mg L^{-1}, a 969% increase in concentration.

Trends in material loads for DIN and NO_3-N within Lost Creek followed those observed for their respective concentrations, increasing in reaches I and II followed by declines in reaches III and IV (Fig. 4c-d). On average, DIN load increased from 3.09 to 16.96 kg d^{-1} (i.e., 448%) over the length of Lost Creek. Trends in DIN reflected changes in in NO_3-N, as the loads of NH_4-N were comparatively small (0.87 ± 0.22 kg d^{-1}) and had no observable temporal or spatial trend (Fig. 4d).

Dissolved inorganic N in spring brooks and irrigation diversions was dominated by NO_3-N as concentrations of NH_4-N were consistently low (< 0.015 mg L^{-1}, Fig. S5a, c, e). Among spring brooks, however, NO_3-N concentrations varied greatly with values ranging from 0.032-0.585 mg N L^{-1}; the greatest concentrations of DIN among all the lotic sampling sites, 0.417 ± 0.045 mg L^{-1} and 0.483 ± 0.037 mg L^{-1} (grand mean ± standard error), were found in spring brooks S1 and S2, respectively.

Because of lower flows and variable N content, loads of DIN and NO_3-N associated with spring brooks and irrigation diversions were generally smaller than those associated with sites within Lost Creek (Fig. S5b, d). The exception to this was spring brook S2, which consistently transported large amounts of DIN (predominantly NO_3-N) into Reach I of Lost Creek (12.29 ± 0.91 kg N d^{-1}, mean ± standard error) representing 80% of the N load entering the reach. In comparison, spring brook S3 and S4 together transported only 2.97 ± 0.56 kg N d^{-1} of DIN into Reach II of Lost Creek, constituting 36% of N inputs. Due to much lower concentrations, loads of NH_4-N were an order of magnitude lower than those for NO_3-N (Fig. S5f).

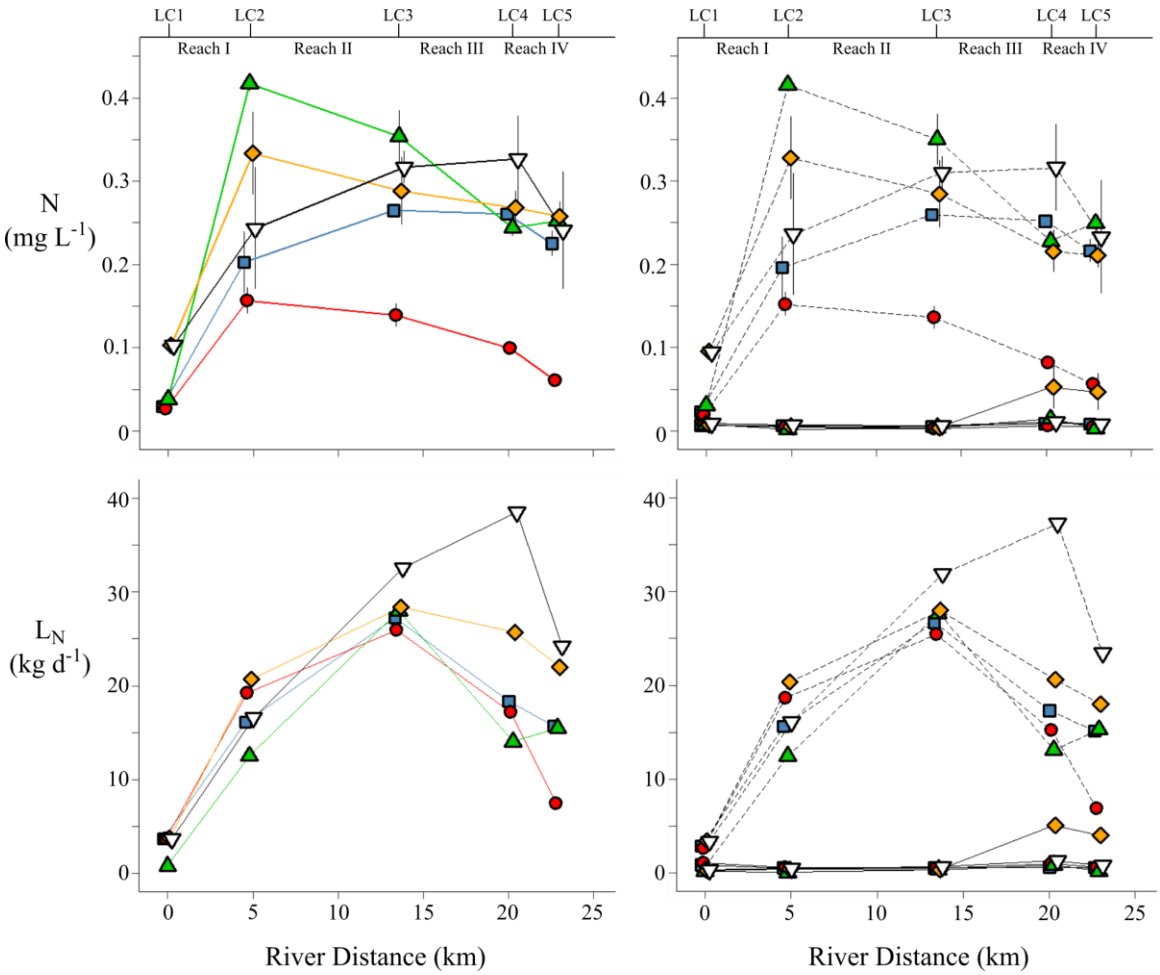

Figure 4: Concentrations of DIN (a) and individual N species (b) and their respective loads (c, d) at five sites (LC1-LC5) that bound the four reaches in Lost Creek. Reaches are delineated along the top of panels a and b. Points are colored by the sampling date and plotted against river distance from LC1. Data are means ± standard error.

3.4 Spatiotemporal Patterns in Cl Concentration

Chloride concentrations changed significantly with distance downstream as Lost Creek proceeded from sites up-gradient of the WWHP ponds (e.g., LC1, Fig. 1) to more downstream locations (Fig. 5a). Concentrations of Cl in water that flows into the studied section of Lost Creek were low (< 2 mg L^{-1}) but increased 265% after transport through reaches I and II. Further increase occurred within Reach III (0.74 ± 0.22 mg L^{-1}), but generally Cl concentrations remained fairly constant through the downstream reaches after increases observed in reaches I and II. On average, Cl concentrations increased by 307% over the length of Lost Creek. Mean concentration of Cl in spring brooks (6.34 ± 0.39 mg L^{-1}, Fig. 5b) was higher than that in Lost Creek (4.42 ± 0.39 mg L^{-1}).

Concentrations of Cl and NO_3-N were both consistently low at the most upstream site (LC1, located upgradient of the infiltration bed, Fig. 5c) and these analytes increased in tandem with distance downstream ($r = 0.80$, $p < 0.001$). When data were restricted to surface samples collected from the consistently gaining reaches (i.e., reaches I and II) Cl and NO_3-N concentrations were even more closely related ($r = 0.96$ $p < 0.001$).

Wells directly downgradient of the infiltration beds had concentrations of NO_3-N and Cl on average 6.40 and 19.33 mg L^{-1}, respectively, from June 2019 to February 2021 (Elizabeth Erickson, Water and Environmental Technologies, pers comm). Whereas, surface and groundwater directly upgradient of these infiltration bed had concentrations of NO_3-N and Cl generally below 0.1 mg L^{-1} and 2 mg L^{-1}, respectively.

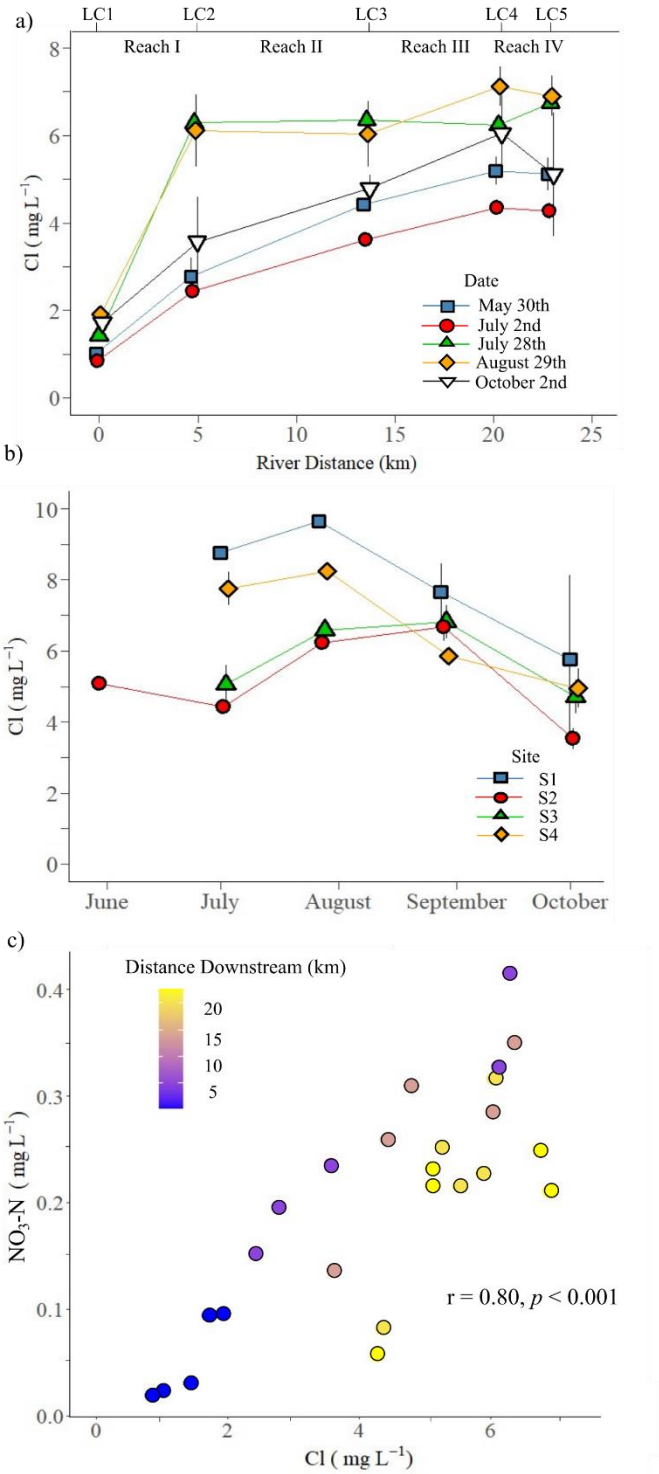

Figure 5: Chloride concentrations (mg L^{-1}) at the five channel sites along Lost Creek (a) and four spring brooks (b), and the relationship between NO_3-N and Cl concentrations for surface water collected from Lost Creek's five monitoring sites across 5 sampling dates. Points are color coded based upon the sampling date (a), sampling site (b), and site distance downstream from the most upstream site, LC1 (c). Data are means ± standard error. Error bars in panel c are not included.

388

3. 5 Change in Load, Groundwater Exchange, and Biogeochemical Processing

Individual study reaches showed temporally consistent patterns of net DIN accumulation or removal throughout the sampling season that differed among reaches ($p < 0.05$, Fig. 6). Mean ΔL_{DIN} in reaches I (20.08 ± 1.58 kg N d^{-1}) and II (10.63 ± 1.92 kg N d^{-1}) were positive and different than zero ($p < 0.05$, Fig. 6a). Increases in DIN load were mainly due to groundwater inputs. In the gaining reaches, $\Delta L_{gw\ DIN}$ averaged 18.35 ± 1.74 and 10.89 ± 1.50 kg N d^{-1} and represented 91.6 and 95.2 % of inputs in reaches I and II, respectively (Fig. 6b). Positive mean values for $\Delta L_{bio\ DIN}$ in reaches I and II (1.73 ± 0.85 and 0.53 ± 2.63 kg N d^{-1}, respectively, Fig. 6c) were not different than zero ($p > 0.05$) and represented only 9.4 and 4.8% of DIN inputs. Reaches III and IV exhibited the opposite trend to that observed in reaches I and II; means for ΔL_{DIN} in reaches III and IV were, similar, negative (-5.96 ± 3.49 and -5.50 ± 2.76 kg N d^{-1}, respectively), and not different than zero ($p > 0.05$). Both biotic uptake and hydrologic losses reduced DIN load in reaches III and IV, with $\Delta L_{bio\ DIN}$ representing 62.4 and 73.5% of total losses, respectively. However, neither mean $\Delta L_{bio\ DIN}$ nor $\Delta L_{gw\ DIN}$ within reaches III and IV were different than zero ($p > 0.05$).

Nitrate accumulation or removal within Lost Creek mimicked that of DIN but showed marked differences in its partitioning between ΔL_{gw} and ΔL_{bio}. Mean ΔL_{NO3} was positive and different than zero ($p < 0.05$) for reaches I and II (19.97 ± 1.56 and 11.33 ± 1.87 kg N d^{-1}, respectively, Fig. 6d) with increases in NO_3-N due to significant load change ($p < 0.05$) from both ΔL_{gw} and ΔL_{bio}. Greater NO_3-N load was derived from groundwater (14.93 ± 1.20 kg N d^{-1}, Fig. 6e) compared to biotic production (4.61 ± 0.81 kg N d^{-1}, Fig. 6f) in Reach I and comparable rates of input (5.53 ± 0.94 vs 5.46 ± 1.94 kg N d^{-1}) from these respective sources occurred in Reach II. In reaches III and IV, mean ΔL_{NO3} was negative (-7.27 ± 3.45 and -4.95 ± 2.77 kg N d^{-1}, respectively), but loads declined significantly ($p < 0.05$) only in Reach III related to negative measures for $\Delta L_{gw\ NO3}$ (-2.60 ± 1.57 kg N d^{-1}, $p < 0.05$).

Mean ΔL_{NH4} for all reaches was an order or magnitude lower than ΔL_{DIN} and ΔL_{NO3}, and only the decline in Reach IV (-0.518 ± 0.152 kg N d^{-1}) was different from zero ($p < 0.05$, Fig. 6g). Load change

associated with groundwater exchange ($\Delta L_{gw\ NH4}$) and biogeochemical processing ($\Delta L_{bio\ NH4}$) were of similar magnitude but with different influences on ΔL_{NH4} (Fig. 6h-i). Mean values for $\Delta L_{gw\ NH4}$ were positive (3.218 and 5.852) and different from zero in the upstream gaining reaches (Reach I and II, respectively, $p < 0.05$). Measures of $\Delta L_{bio\ NH4}$, however, were negative (-2.891 and -4.961) and different from zero ($p < 0.05$) in the same reaches. In reaches III and IV, neither load changes due to groundwater exchange ($\Delta L_{gw\ NH4}$) nor biogeochemical processing ($\Delta L_{bio\ NH4}$) were different from zero (Fig. 6i, $p > 0.05$).

Dissolved inorganic N load accumulated (20.03 ± 3.50 kg N d^{-1}, 4.7-fold) along the length of Lost Creek primarily reflecting a more than 5-fold increase in NO_3-N mass transport (19.08 ± 3.33 kg N d^{-1}). Changes in NH_4-N loads (0.95 ± 0.67 kg N d^{-1}) were not significant ($p > 0.05$, Fig. S6). Groundwater input of DIN (25.53 ± 2.65 kg N d^{-1}) was the dominant N source to the system, mainly importing NO_3-N (17.19 ± 1.14 kg N d^{-1}) but with 33% of load increase composed of NH_4-N (8.43 ± 1.88 kg N d^{-1}). Different directions of load change due to biogeochemical processing occurred among the sampling dates and means values were generally not different than zero across the N species except for significant ($p < 0.05$) removal of NH_4-N (Fig. S6).

434

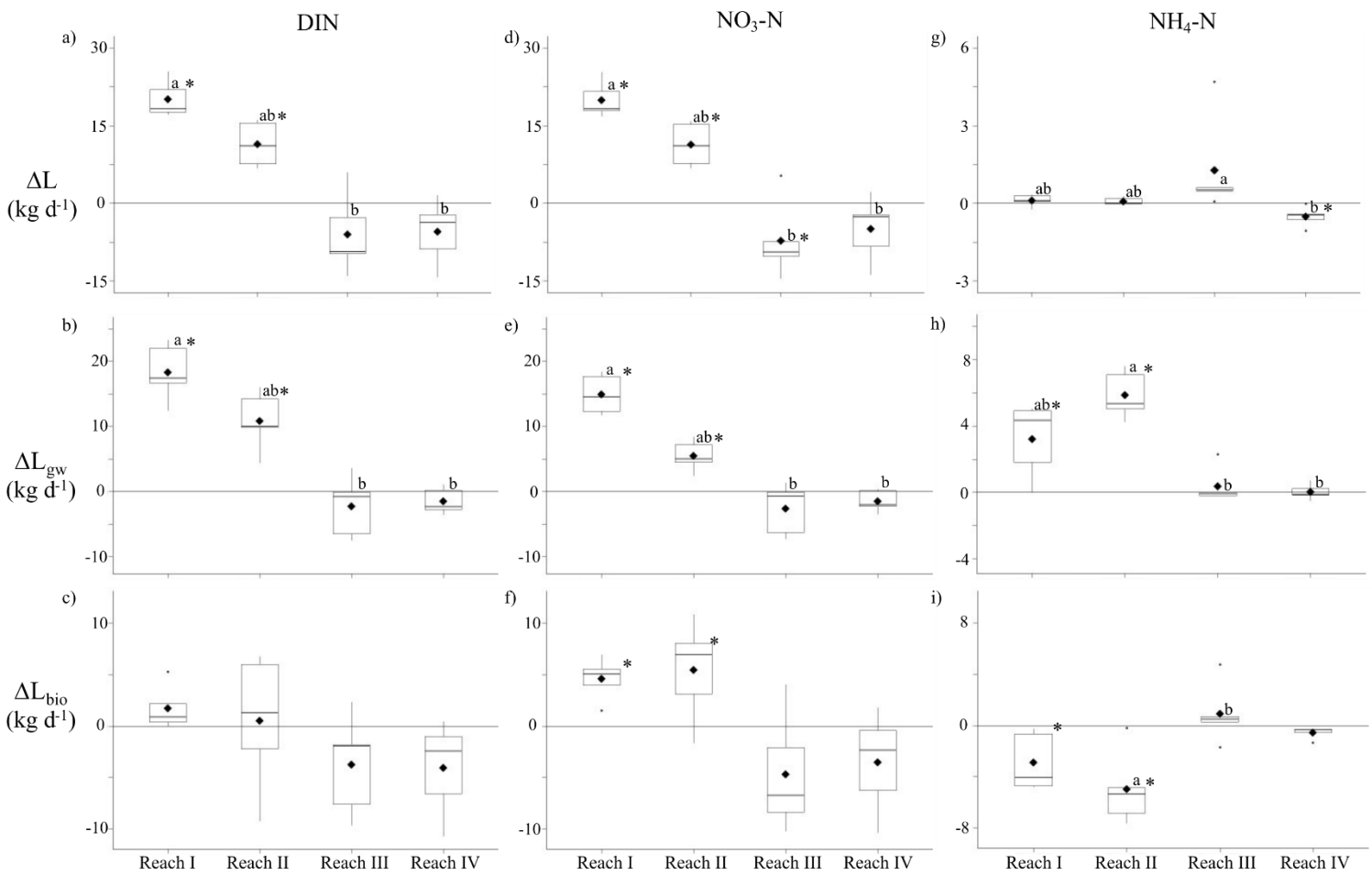

Figure 6: Net change in nitrogen loads (ΔL) partitioned by groundwater exchange (ΔL_{gw}) and biogeochemical processing (ΔL_{bio}) within each reach across all sampling dates for DIN (a, b, c), NO_3-N (d, e, f) and NH_4-N (g, h, i). Boxplots include the 25th and 75th percentiles (box limits), median (central line), values in the lowest and highest quartiles (whiskers), significant outliers (exceeding the absolute value of the 25th or 75th quartiles minus 1.5-times the interquartile range), and the mean (black diamond). Distinct alphabetical superscripts indicate reaches that behave differently ($p < 0.05$) according to multiple comparison test among reaches after a Kruskal-Wallis rank sum test and asterisks indicate the mean value is significantly ($p < 0.05$) different from zero following one-sample location t-tests.

Reflecting patterns of ΔL_{bio}, the effective solute fluxes for N species (U_{bio}) differed substantially among the four stream reaches along the length of Lost Creek (Fig. 7, Table S2). Reach I and II consumed NH_4-N and had similar and largest flux magnitude for this N species (-135.30 ± 42.12 and -113.253 ± 26.52 mg N m^{-2} d^{-1}, respectively, $p < 0.05$). Further, both Reach I and II were significant ($p < 0.05$) net producers of NO_3-N. $U_{bio\text{-}NO3}$ was maximal in Reach I (215.79 ± 38.10 mg N m^{-2} d^{-1}) and in excess of observed negative values for $U_{bio\text{-}NH4}$ in the same reach. In Reach II, $U_{bio\text{-}NO3}$ (124.66 ± 44.24 mg N m^{-2} d^{-1}) was very similar in magnitude to the effective NH_4-N consumption rate. Reach IV also consumed NH_4-N but to a lesser degree (-55.89 ± 20.51 mg N m^{-2} d^{-1}, $p < 0.05$), whereas $U_{bio\text{-}NH4}$ was not different from zero in Reach III ($p > 0.05$). In contrast to the biogeochemical production of NO_3-N characteristic of reaches I and II, effective solute fluxes for NO_3-N in reaches III and IV were strongly negative but large temporal variation resulted in mean values not different from zero ($p > 0.05$). Combined fluxes for NH_4-N and NO_3-N revealed significant ($p < 0.05$) net DIN production in Reach I (81.17 ± 40.17 mg N m^{-2} d^{-1}), but no significant change in DIN in any of the other stream reaches.

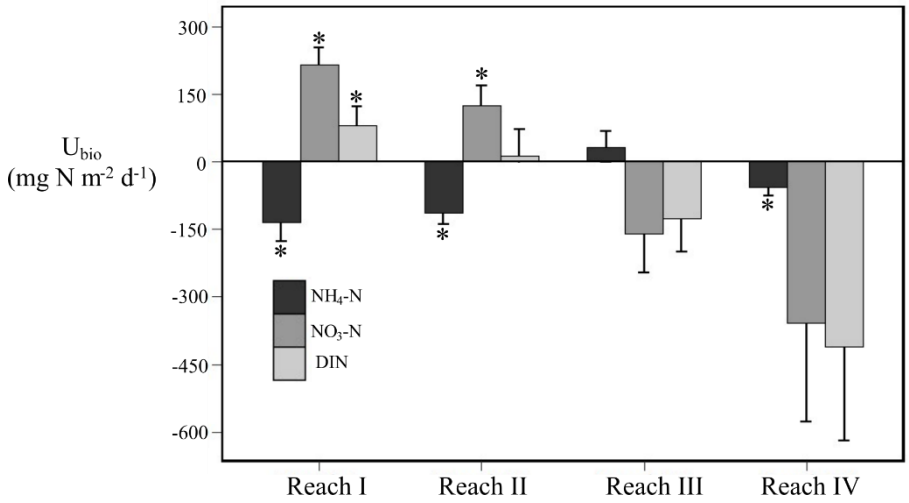

Figure 7: Effective biogeochemical flux (U_{bio}, mg N m^{-2} d^{-1}) for NH_4-N, NO_3-N, and DIN for reaches I-IV across the five sampling dates. Data are means + standard errors (n = 5). Asterisks indicate mean values are significantly different ($p < 0.05$) from zero following one-sample location t-tests.

457

458

459

3.6 Fen Characterization and Influence

The fen covers ca. 1.26 km^2 with organic deposit depths averaging 1.72 m (limits = 0.43-3.09 m). Hydraulic conductivity of the fen averaged 2.19 m d^{-1} with minimum and maximum values of 0.006 and 12.56 m d^{-1}. The fen was increasingly dewatered over the course of the growing season (Fig. S7); approximately 87.5% of the fen volume was saturated at the end of May and maximum dewatering was observed in late August when only 56.1% of the fen was saturated with water. Dewatering within the fen was spatially variable, with some portions remaining fully saturated at all times and other areas experiencing water table decline of up to 2 m (Fig. S7).

The Dutchman Fen minimally affected N transport to Lost Creek. Volumetric flow through the fen varied from 0.24 – 0.41 L s^{-1} with an average of 0.30 L s^{-1}, values that are more than 1500-fold less than the average Q_{gw} in reaches I and II (Fig. 3). Flowtubes within the fen had weak and differing influences on the load of DIN (Fig. 8a); ΔL_i values ranged from -0.007 to 0.001 kg N d^{-1}. Only the third flow tube had a significant influence on DIN load (-0.0004 ± 0.0001 kg N d^{-1}, $p < 0.05$). Overall, the fen had little influence on DIN transport; mean ΔL_F was -0.0017 ± 0.001 kg N d^{-1}, a change not different than zero ($p > 0.05$). The average groundwater input of DIN ($\Delta L_{GW\ DIN}$, 25.95 ± 2.47 kg N d^{-1}) into Lost Creek was 1338-fold larger than mean ΔL_F ($p < 0.05$, Fig. 8b) over the course of the five sampling dates.

478

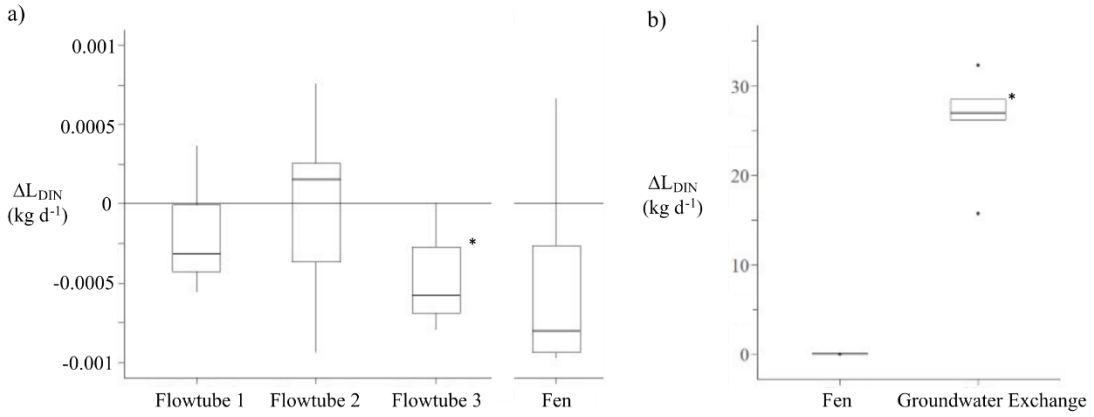

Figure 8: a) Change in DIN load within each flowtube (ΔL_i) and the fen as a whole (ΔL_F) among all sampling dates with outliers removed. b) Change in DIN load due to the fen and groundwater exchange (ΔL_{GW}) among all sampling dates. Boxplots include the 25th and 75th percentiles (box limits), median (central line), values in the lowest and highest quartiles (whiskers), and significant outliers (exceeding the absolute value of the 25th or 75th quartiles minus 1.5-times the interquartile range). Asterisks indicate the mean value is significantly different than zero.

4.0 DISCUSSION

The chemical composition of channel water in low-order streams is dictated by the transport of landscape-derived materials and internal biogeochemical processes that alter the form and abundance of the imported solutes. The magnitude of influence between transport and processing changes longitudinally along a stream creating unique domains of behavior (Montgomery et al. 1999, Thorp et al. 2006). This study illustrated that spatially-distinct domains were observed within Lost Creek, with some having greater influence on overall stream water composition as a result of N import associated with localized zones of groundwater discharge. Lost Creek's internal biogeochemical processing played relatively little role in altering N loads but was influential in dictating its form. Biogeochemical processing consumed NH_4^+ and generated NO_3^- likely reflecting nitrification at the stream-groundwater interface. Thus, the transport of landscape-derived solutes dictated N abundance within Lost Creek reflecting extensive connectivity between the systems manifested as substantial groundwater discharge. Landscape inputs of N to Lost Creek were not influenced by the Dutchman Fen, but appear linked to the disposal of treated municipal effluent.

4.1 Groundwater-Surface Water Linkage Influence on Lost Creek

Trends in DIN concentration and loads within Lost Creek were directly linked to the relative magnitudes of groundwater input. Water entering the study system was characterized by low DIN concentrations consistent with relatively pristine conditions in the upper watershed. Reaches I and II receive substantial inputs of DIN via groundwater discharge that resulted in increases in NO_3^- concentration and loads. In contrast, downstream reaches either receive minimal groundwater inputs or lose surface water to the groundwater system. Although measured fluxes of biogeochemical removal of NO_3^- and NH_4^+ (Negative $U_{bio\ NO3}$ and $U_{bio\ NH4}$) were in the upper range of values reported in the Lotic Intersite N eXperiments (LINX I and II; Webster et al. 2003, Mulholland et al. 2008) and were comparable to uptakes rates observed in N-saturated streams (Earl et al. 2006, O'Brien et al. 2007), they were not commensurate within groundwater N inputs. So, whilst internal biogeochemical processing and

advective transport of NO_3^- to the groundwater system in downstream reaches resulted in declining DIN concentration and load reduction, Lost Creek's N abundance remained elevated due to groundwater N inputs.

Although groundwater inputs clearly influence abundance of N within Lost Creek, its influence appears to vary depending on the time of year. Indeed, the fraction of water within a stream derived from nearby groundwater sources, as compared to upstream channel flow, can fluctuate due to peak flow events (Covino and McGlynn 2007), resulting in alterations of N abundance within the channel (Burns et al. 1998b). In late May and early July, concentrations of NO_3^- were lower at several sites compared to later sampling dates. On these sampling dates, Lost Creek experienced greater magnitudes of channel flow from upstream in comparison to groundwater discharge, likely reflecting the influences of snowmelt. Increased relative channel flow potentially caused a dilution of groundwater DIN inputs resulting in lower concentrations of NO_3^- observed within the stream. This is further supported by fairly stable ΔL_{DIN} within Lost Creek, suggesting similar net inputs of DIN via groundwater, but variable concentrations of NO_3^- as a result of mixing and dilution with upstream water.

4.2 Instream Nitrification

Lost Creek's channel-groundwater interface appears to act as a hotspot of nitrification reflecting the import of NH_4^+ rich groundwater and active biogeochemical processing. Ammonium transported via diffuse groundwater input to the interface with well-oxygenated waters of Lost Creek appears to then be nitrified, enhancing NO_3^- loads in gaining reaches. The proposed occurrence of nitrification is supported by the lack of NH_4^+ within Lost Creek, the significant and congruent biogeochemical removal of NH_4^+ and production of NO_3^- within gaining reaches, and the magnitudes and directions of effective solute fluxes $U_{bio\text{-}NH4}$ and $U_{bio\text{-}NO3}$. The magnitude of net nitrification within Lost Creek (obtained from positive $U_{bio\ NO3}$ values) exhibited a broad range of values, but suggest significant rates of NH_4^+ transformation. The lower rates of nitrification reported here were similar to those found in non-polluted low-order streams (Grimm et al. 1991, Hamilton et al. 2001, Brookshire et al. 2005). However, the average rate of

net nitrification within Lost Creek's reaches were an order of magnitude larger than those previously reported for non-polluted stream systems, and were similar to values found within N-enriched streams receiving anthropogenic inputs from agriculture (O'Brien et al. 2007).

The net nitrification observed within Lost Creek cannot be accounted for solely by the conversion of groundwater imported NH_4^+. This is especially the case in Reach I, where the absolute value of $U_{bio\ NO3}$ is 1.6-fold larger than that accounted for by negative $U_{bio\ NH4}$ values, suggesting an additional source of NH_4^+. Mineralization and nitrification of in-situ organic N could be contributing to this excess NO_3^- production (Starry et al. 2005). Potential sources of organic N within Lost Creek include more extensive wetlands and an artificial pond associated with reaches I and II that have deposits of organic material and the stream bed itself that supports mats of attached macrophytes. In addition, import of dissolved organic matter (DOM) from the landscape may be a source of organic N. Wetlands have been shown to export DOM to nearby stream systems (Lottig et al. 2013) and while DOM N content varies (Petrone et al. 2009, Watanabe et al. 2014) significant fractions of DOM removal have been associated with in-stream mineralization and nitrification (Brookshire et al. 2005). The LCDC landscape contains an extensive wetland area, closely associated with upstream reaches, that is characterized by high groundwater DOC concentrations. Wetland-derived DOC is transported into Lost Creek by groundwater discharge within reaches I and II wherein biotic activity may result in mineralization and release of inorganic N.

4.3 Fen Influence on Stream N Abundance

Although wetlands have been shown to alter stream N abundance (Devito et al. 1989, Rücker and Schrautzer 2010, Cheng et al. 2020), the Dutchman Fen does not appear to notably influence Lost Creek. The observed seasonal dewatering in the fen did not appear to result in net mineralization of N within the fen. Seasonal dewatering could be attributed to irrigation withdrawals and/or the combination of decreased precipitation and enhanced evapotranspiration as the growing season progresses. Instead of acting as a source for N, the Dutchman Fen did little to alter N loads.

553 Variability in wetland form and function can be summarized by the difference in their ability to
554 transport water and their influence on N (Brinson 1993). The observed lack of N mass removal can be
555 attributed to the fen's low hydraulic conductivity resulting in minimal transport of water. Maximal N
556 removal occurs when the rate of reaction matches the rate of transport (Ocampo et al. 2006, Harvey et al.
557 2013, Oldham et al. 2013). The fen may have a high potential for N removal owing to abundant plant
558 cover, organic-rich saturated materials, and near anoxic conditions. However, for the Dutchman fen,
559 observed mass of N removed appears to be minimized by the low rates at which water and N are
560 transported through the system. At a broader landscape scale, fens may serve a minimal role in altering
561 water quality owing to peat often having low substrate permeability (Wong et al. 2009, Rezanezhad et al.
562 2016).

563 **4.4 Local-Intermediate Groundwater System**

564 As rivers move from alpine montane environments to valley bottoms, they generally lose water as
565 seepage to the underlying groundwater system (Niswonger et al. 2005, Covino and McGlynn 2007). This
566 seepage, along with groundwater recharge from the adjacent mountain block, can discharge in discrete
567 zones within the valley bottom forming springs (Mayo et al. 2003) and basin riparian zones (Wilson and
568 Guan 2004). Stable groundwater flowpaths, steady spring brook flow, and the consistent and large
569 groundwater inputs into reaches I and II, suggest that upstream portions of Lost Creek are being fed by
570 long intermediate flowpaths linked to the adjacent mountain system. These intermediate flowpaths may
571 be responsible for the creation and maintenance of the extensive wetland complex and the Dutchman Fen
572 within the LCDC.

573 Results of our mass-balance assessment suggest that this intermediate flowpath is being polluted by
574 the nearby municipal effluent infiltration beds before water discharges into Lost Creek. I observed
575 elevated concentrations of DIN and Cl within the groundwater system, spring brooks, and sites within
576 Lost Creek downgradient of the effluent infiltration beds. In addition, concentrations of NO_3^- rise
577 concomitantly with Cl concentrations as Lost Creek flows through the LCDC, especially within reaches I

578 and II that are directly downgradient of the infiltration beds and receive the majority of groundwater
579 inputs. The only known source of Cl in the area is from the municipal effluent. Potash fertilizer
580 (potassium Cl) has not been applied to several of the adjacent agricultural fields within the last 10 years
581 (Thomas Heggelund, Farmer/Rancher, pers comm). In addition, there is no evidence of abundant Cl
582 containing rocks within geologic surveys conducted in the region (Wanek and Barclay 1966, Konizeski et
583 al. 1968). Increased Cl concentrations have been used as an indicator of municipal wastewater release
584 (Gasser et al. 2010). Thus, the concurrent elevation of NO_3^- and Cl concentrations within Lost Creek
585 strongly suggests that municipal effluent is entering Lost Creek, and is the source of N pollution to the
586 groundwater system.

587 The major form of DIN in the effluent plume directly downgradient of the infiltration ponds is NO_3^-.
588 In contrast, groundwater DIN was dominated by NH_4^+, even though Cl concentrations were elevated
589 throughout the piezometer network suggesting effluent-derived N. The asymmetry in N form between the
590 effluent plume and groundwater discharging to Lost Creek may be attributed to dissimilatory NO_3^-
591 reduction to NH_4^+ (DNRA). The microbial mediated process of DNRA transforms NO_3^- to NH_4^+ and is
592 thought of to occur predominantly in anoxic environments that contain an abundance of organic carbon
593 (Tiedje 1988, Burgin et al. 2007). The extensive wetland complex in the LCDC is rich in organic
594 material, contains high concentrations of DOC, and presumably microsites of anoxia, making it an ideal
595 site for DNRA. As the effluent plume reaches the wetland soils, some NO_3^- may be removed by
596 denitrification, but it appears that substantial amounts are reduced to NH_4^+ via DNRA, remaining
597 available for further transport towards Lost Creek. Nitrate within a landfill has previously been shown to
598 be converted to NH_4^+ via DNRA due to plume interaction with abundant organic matter (Bulger et al.
599 1990). Microbial use of NO_3^- for DNRA instead of denitrification reduces the efficiency of N removal
600 within the system and may be in part responsible for the continued transport of N pollution to Lost Creek
601 and the UCFR.

602

5.0 Conclusion

This study elucidated the drivers of N concentration and load within Lost Creek to better understand the influence groundwater-surface water has on system material processing. Using a mass-balance approach, I was able to quantify the transport and biogeochemical processing of N at various spatial and temporal scales. I identified that: 1) groundwater exchange is dictating the abundance of N within Lost Creek; 2) groundwater inputs of N to Lost Creek appear to be derived from municipal effluent; and 3) the Dutchman Fen does little to alter N loads within the groundwater system. These findings highlight the significance of longitudinal alterations in the linkage-strength between surface and groundwater systems. Points of strong interaction between these systems can have consequences for stream water quality and N abundance, especially for low-order streams owing to their relatively small size. These points of interaction may have disproportionate influence on the system as a whole as the stream's internal removal processes become saturated, resulting in propagation of N pollution downstream. Although biogeochemical removal of N in Lost Creek was not commensurate with N import, it was instrumental in dictating the form of inorganic N within the system.

The mass-balance approach applied here provides a robust framework that can be applied to a variety of other systems with nutrient pollution issues. Understanding sources of nutrient pollution to a given system as well as the capacity of a system to processes imported nutrients is critical knowledge for developing restoration, remediation, and management plans.

6.0 References Cited

Applied Ecological Services. 2011. Supplementary Vegetation 2011 Report for the Dutchman Riparian Lands. Deer Lodge County, Montana. J:110431:061512 Brodhead, Wisconsin.

Baillieux, A., Campisi, D., Jammet, N., Bucher, S. and Hunkeler, D., 2014. Regional water quality patterns in an alluvial aquifer: Direct and indirect influences of rivers. Journal of contaminant hydrology 169:23-131.

Barton, D. 2018. Permit Fact Sheet Montana Groundwater Pollution Control Services. Montana Department of Environmental Quality Water Protection Bureau, Helena MT

Bennett, R. 1962, Flownet analysis. In J. G. Ferris, D.B. Knolwles, R. H. Borwn, and R. W. Stallman (eds.), Theory of Aquifer Test. U.S. Geol. Surv. Prof. Paper 708:70

Böhlke, J.K. and Denver, J.M. 1995. Combined use of groundwater dating, chemical, and isotopic analyses to resolve the history and fate of nitrate contamination in two agricultural watersheds, Atlantic coastal plain, Maryland. Water Resources Research. 31:2319-2339.

Bouwer, H. and Rice, R.C., 1976. A slug test for determining hydraulic conductivity of unconfined aquifers with completely or partially penetrating wells. Water resources research 12:423-428.

Bouwer, H., 1989. The Bouwer and Rice Slug Test—An Update a. Groundwater 27:304-309.

Brookshire, E. N. J., Valett, H. M., Thomas, S. A., and Webster, J. R. 2005. Coupled cycling of dissolved organic nitrogen and carbon in a forest stream. Ecology 86:2487-2496.

Brown, B. V., Valett, H. M., and Schreiber, M. E., 2007. Arsenic transport in groundwater, surface water, and the hyporheic zone of a mine-influenced stream-aquifer system. Water Resources Research 43.

Bulger, P.R., Kehew, A.E. and Nelson, R.A., 1989. Dissimilatory nitrate reduction in a waste-water contaminated aquifer. Groundwater 27:664-671.

Burgin, A.J. and Hamilton, S.K., 2007. Have we overemphasized the role of denitrification in aquatic ecosystems? A review of nitrate removal pathways. Frontiers in Ecology and the Environment, 5:.89-96.

Burns, D. A., 1998a. Retention of NO_3^- in an upland stream environment: A mass balance approach. Biogeochemistry 40:73-96.

Burns, D.A., Murdoch, P.S., Lawrence, G.B. and Michel, R.L., 1998b. Effect of groundwater springs on NO3− concentrations during summer in Catskill Mountain streams. Water Resources Research 34:1987-1996.

Carey, R. O., and Migliaccio, K. W., 2009. Contribution of wastewater treatment plant effluents to nutrient dynamics in aquatic systems: a review. Environmental Management 44:205-217.

Casagrande, A., 1937. Seepage through dams. Journal of New England Water Works 51:295-336

Chestnut, T.J. and McDowell, W.H., 2000. C and N dynamics in the riparian and hyporheic zones of a tropical stream, Luquillo Mountains, Puerto Rico. Journal of the North American Benthological Society 19:199-214.

Cirmo, C. P., and McDonnell, J. J. 1997. Linking the hydrologic and biogeochemical controls of N transport in near-stream zones of temperate-forested catchments: a review. Journal of Hydrology 199:88-120.

Clément, J.C., Aquilina, L., Bour, O., Plaine, K., Burt, T.P. and Pinay, G. 2003. Hydrological flowpaths and nitrate removal rates within a riparian floodplain along a fourth-order stream in Brittany (France). Hydrological processes, 17:1177-1195.

Covino, T. P., and McGlynn, B. L., 2007. Stream gains and losses across a mountain-to-valley transition: Impacts on watershed hydrology and stream water chemistry. Water Resources Research 43.

Correll, D.L., Jordan, T.E. and Weller, D.E., 1992. Nutrient flux in a landscape: effects of coastal land use and terrestrial community mosaic on nutrient transport to coastal waters. Estuaries, 15:431-442.

Devito, K.J., Dillon, P.J. and Lazerte, B.D., 1989. Phosphorus and nitrogen retention in five Precambrian shield wetlands. Biogeochemistry 8:185-204.

669 Dodds WK and Welch EB. 2000. Establishing nutrient criteria in streams. Journal of the North American
670 Benthological Society 19:186–196

671 Dodds, W.K. and Smith, V.H., 2016. Nitrogen, phosphorus, and eutrophication in streams. Inland Waters
672 6:155-164.

673 Doulatyari, B., Betterle, A., Basso, S., Biswal, B., Schirmer, M. and Botter, G., 2015. Predicting
674 streamflow distributions and flow duration curves from landscape and climate. Advances in Water
675 Resources 83:285-298.

676 Duff, J. H., Tesoriero, A. J., Richardson, W. B., Strauss, E. A., and Munn, M. D., 2008. Whole-stream
677 response to nitrate loading in three streams draining agricultural landscapes. Journal of Environmental
678 Quality 37:1133-1144.

679 Earl, S.R., Valett, H.M. and Webster, J.R., 2006. Nitrogen saturation in stream ecosystems. Ecology
680 87:3140-3151.

681 Esri Inc. 2020. ArcMap (Version 10.6.1). Esri Inc. https://www.esri.com/en us/arcgis/products/arcgis-
682 pro/.

683 Fabre, C., Sauvage, S., Guilhen, J., Cakir, R., Gerino, M., and Sánchez-Pérez, J. M., 2020. Daily
684 denitrification rates in floodplains under contrasting pedo-climatic and anthropogenic contexts:
685 modelling at the watershed scale. Biogeochemistry 149:317-336.

686 Galloway, J.N., Dentener, F.J., Capone, D.G., Boyer, E.W., Howarth, R.W., Seitzinger, S.P., Asner, G.P.,
687 Cleveland, C.C., Green, P.A., Holland, E.A. and Karl, D.M., 2004. Nitrogen cycles: past, present, and
688 future. Biogeochemistry 70:153-226.

689 Gasser, G., Rona, M., Voloshenko, A., Shelkov, R., Tal, N., Pankratov, I., Elhanany, S. and Lev, O.,
690 2010. Quantitative evaluation of tracers for quantification of wastewater contamination of potable
691 water sources. Environmental science & technology 44:3919-3925.

692 Gilmore, T.E., Genereux, D.P., Solomon, D.K., Solder, J.E., Kimball, B.A., Mitasova, H. and Birgand, F.,
693 2016. Quantifying the fate of agricultural nitrogen in an unconfined aquifer: Stream-based
694 observations at three measurement scales. Water Resources Research 52:1961-1983.

695 Giraudoux, P., 2021. pgirmess: Spatial Analysis and Data Mining for Field Ecologists. R package version
696 1.7.0. https://CRAN.R-project.org/package=pgirmess

697 Green, C.T., Puckett, L.J., Böhlke, J.K., Bekins, B.A., Phillips, S.P., Kauffman, L.J., Denver, J.M. and
698 Johnson, H.M., 2008. Limited occurrence of denitrification in four shallow aquifers in agricultural
699 areas of the United States. Journal of Environmental Quality 37:994-1009.

700 Grimm, N.B., Valett, H.M., Stanley, E.H. and Fischer, S.G., 1991. Contribution of the hyporheic zone to
701 stability of an arid-land stream. Internationale Vereinigung für theoretische und angewandte
702 Limnologie: Verhandlungen 24:1595-1599.

703 Gu, C., Hornberger, G.M., Herman, J.S. and Mills, A.L., 2008. Influence of stream-groundwater
704 interactions in the streambed sediments on NO3− flux to a low-relief coastal stream. Water Resources
705 Research 44.

706 Hamdhani, H., Eppehimer, D. E., and Bogan, M. T., 2020. Release of treated effluent into streams: A
707 global review of ecological impacts with a consideration of its potential use for environmental flows.
708 Freshwater Biology 65:1657-1670.

709 Hamilton, S. K., J. L. Tank, F. David, W. M. Wollheim, B. J. Peterson, and J. R. Webster. 2001. Nitrogen
710 uptake and transformation in a Midwestern U.S. stream: A stable isotope enrichment study.
711 Biogeochemistry 54:297–340.

712 Harvey, J. W., Böhlke, J. K., Voytek, M. A., Scott, D., and Tobias, C. R. (2013). Hyporheic zone
713 denitrification: Controls on effective reaction depth and contribution to whole-stream mass
714 balance. Water Resources Research 49:6298-6316.

715 Hey, D.L., Kostel, J.A., Crumpton, W.G., Mitsch, W.J. and Scott, B., 2012. The roles and benefits of
716 wetlands in managing reactive nitrogen. Journal of Soil and Water Conservation 67:47-53.

717 Howarth, R.W., Billen, G., Swaney, D., Townsend, A., Jaworski, N., Lajtha, K., Downing, J.A., Elmgren,
718 R., Caraco, N., Jordan, T. and Berendse, N.F., 1996. Riverine inputs of nitrogen to the North Atlantic
719 Ocean: fluxes and human influences. Biogeochemistry 35:75-139.

720 Howarth, R., Swaney, D., Billen, G., Garnier, J., Hong, B., Humborg, C., Johnes, P., Mörth, C.M. and
721 Marino, R., 2012. Nitrogen fluxes from the landscape are controlled by net anthropogenic nitrogen
722 inputs and by climate. Frontiers in Ecology and the Environment 10:37-43.

723 Hurley, P. and Valett., H. 2019. Hydrogeomorphic and biogeochemical assessment of the Lost Creek –
724 Dutchman Complex, Reach A, Upper Clark Fork River, Montana. Natural Resource Damage
725 Program. University of Montana, Missoula, Montana.

726 Ingman, Gary, and Mark A. Kerr. 1990. Nutrient Sources in the Clark Fork River Basin. Clark Fork
727 Symposium Archives.

728 International Organization for Standardization (ISO). 2007. Hydrometry – Measurement of liquid flow in
729 open channels using current-meters or floats. Retrieved from:
730 https://www.iso.org/standard/37573.html. Accessed 3/6/2020.

731 Jencso, K. G., McGlynn, B. L., Gooseff, M. N., Wondzell, S. M., Bencala, K. E., and Marshall, L. A.,
732 2009. Hydrologic connectivity between landscapes and streams: Transferring reach-and plot-scale
733 understanding to the catchment scale. Water Resources Research 45.

734 Jencso, K.G. and McGlynn, B.L., 2011. Hierarchical controls on runoff generation: Topographically
735 driven hydrologic connectivity, geology, and vegetation. Water Resources Research 47.

736 Jones, C. N., D. T. Scott, B. L. Edwards, and R. F. Keim., 2014. Perirheic mixing and biogeochemical
737 processing in flow-through and backwater floodplain wetlands. Water Resources Research 50:7394-
738 7405.

739 Kolbe, T., de Dreuzy, J.R., Abbott, B.W., Aquilina, L., Babey, T., Green, C.T., Fleckenstein, J.H.,
740 Labasque, T., Laverman, A.M., Marçais, J. and Peiffer, S., 2019. Stratification of reactivity
741 determines nitrate removal in groundwater. Proceedings of the National Academy of Sciences,
742 116:2494-2499.

743 Konizeski, R.L., McMurtrey, R.G. and Brietkrietz, A., 1968. Geology and ground-water resources of the
744 Deer Lodge Valley, Montana (No. 1862). US Govt. Print. Off.,.

745 Lottig, N. R., I. Buffam, and E. H. Stanley., 2013. Comparisons of wetland and drainage lake influences
746 on stream dissolved carbon concentrations and yields in a north temperate lake-rich region. Aquatic
747 Sciences 75:619–630.

748 Mayo, A.L., Morris, T.H., Peltier, S., Petersen, E.C., Payne, K., Holman, L.S., Tingey, D., Fogel, T.,
749 Black, B.J. and Gibbs, T.D., 2003. Active and inactive groundwater flow systems: Evidence from a
750 stratified, mountainous terrain. Geological Society of America Bulletin 115:1456-1472.

McDowell, W. H., and Likens, G. E. 1988. Origin, composition, and flux of dissolved organic carbon in the Hubbard Brook Valley. Ecological monographs 58:177-195.

McLatchey, G.P. and Reddy, K.R., 1998. Regulation of organic matter decomposition and nutrient release in a wetland soil. American Society of Agronomy, Crop Science Society of America, and Soil Science Society of America 27:1268-1274

Miltner, R.J. and Rankin, E.T. 1998. Primary nutrients and the biotic integrity of rivers and streams. Freshwater Biology 40:145–158

Mitsch, W.J., Day, J.W., Zhang, L. and Lane, R.R., 2005. Nitrate-nitrogen retention in wetlands in the Mississippi River Basin. Ecological engineering 24:267-278.

Montana Bureau of Mines and Geology Data Center. 2021. Ground Water Information Center.https://mbmggwic.mtech.edu/sqlserver/v11/reports/WellHydrograph.asp?gwicid=5376&agency=mbmg&reqby=M&

Mulholland, P. J., A. M. Helton, G. C. Poole, R. O. Hall, S. K. Hamilton, B. J. Peterson, J. L. Tank, L. R. Ashkenas, L. W. Cooper, C. N. Dahm, W. K. Dodds, S. E. G. Findlay, S. V. Gregory, N. B. Grimm, S. L. Johnson, W. H. McDowell, J. L. Meyer, H. M. Valett, J. R. Webster, C. P. Arango, J. J. Beaulieu, M. J. Bernot, A. J. Burgin, C. L. Crenshaw, L. T. Johnson, B. R. Niederlehner, J. M. O'Brien, J. D. Potter, R. W. Sheibley, D. J. Sobota, and S. M. Thomas. 2008. Stream denitrification across biomes and its response to anthropogenic nitrate loading. Nature 452:202–205.

Niswonger, R.G., Prudic, D.E., Pohll, G. and Constantz, J., 2005. Incorporating seepage losses into the unsteady streamflow equations for simulating intermittent flow along mountain front streams. Water Resources Research 41

O'Brien, J.M., Dodds, W.K., Wilson, K.C., Murdock, J.N. and Eichmiller, J., 2007. The saturation of N cycling in Central Plains streams: 15 N experiments across a broad gradient of nitrate concentrations. Biogeochemistry 84:31-49.

Ocampo, C.J., Oldham, C.E. and Sivapalan, M., 2006. Nitrate attenuation in agricultural catchments: Shifting balances between transport and reaction. Water Resources Research 42.

Oldham, C. E., D. E. Farrow, and Stefan Peiffer. 2013. A generalized Damköhler number for classifying material processing in hydrological systems. Hydrology and Earth System Sciences 17:1133-1148.

Paerl, H. W. 1997. Coastal eutrophication and harmful algal blooms: Importance of atmospheric deposition and groundwater as "new" N and other nutrient sources. Limnology and Oceanography 42:1154–1165.

Pebesma EJ. 2004. Multivariable geostatistics in S: the gstat package. Computers and Geosciences, 30:683-691.

Peterson, B.J., Wollheim, W.M., Mulholland, P.J., Webster, J.R., Meyer, J.L., Tank, J.L., Martí, E., Bowden, W.B., Valett, H.M., Hershey, A.E. and McDowell, W.H. 2001. Control of nitrogen export from watersheds by headwater streams. Science 292:86-90.

Petrone, K. C., Richards, J. S., and Grierson, P. F. (2009). Bioavailability and composition of dissolved organic carbon and nitrogen in a near coastal catchment of south-western Australia. Biogeochemistry, 92(1), 27-40.

Pfeiffer, S. M., Bahr, J. M., and Beilfuss, R. D. (2006). Identification of groundwater flowpaths and denitrification zones in a dynamic floodpain aquifier. Journal of hydrology, 325(1-4), 262-272.

Phillips, P.J., Denver, J.M., Shedlock, R.J. and Hamilton, P.A., 1993. Effect of forested wetlands on nitrate concentrations in ground water and surface water on the Delmarva Peninsula. Wetlands 13:75-83.

Pinay G, Ruffinoni C, Wondzell S, Gazelle F (1998) Change in groundwater nitrate concentration in a large river floodplain:denitrification, uptake, or mixing? J N Am Benthol Soc 17:179–189. https://doi.org/10.2307/1467961

Pretty, J.L., Hildrew, A.G., Trimmer, M., 2006. Nutrient dynamics in relation to surface-subsurface hydrological exchange in a groundwater fed chalk stream. J. Hydrol. 330 (1–2), 84–100.

QGIS Development Team, 2020. QGIS Geographic Information System. Version. 3.12.0 Open Source Geospatial Foundation. URL http://qgis.org

R Core Team 2020. R: A language and environment for statistical computing. Version 4.0.3. R Foundation for Statistical Computing, Vienna, Austria. URL https://www.R-project.org/.

Rezanezhad, F., Price, J.S., Quinton, W.L., Lennartz, B., Milojevic, T. and Van Cappellen, P. 2016. Structure of peat soils and implications for water storage, flow and solute transport: A review update for geochemists. Chemical Geology 429:75-84.

Rivett, M. O., Buss, S. R., Morgan, P., Smith, J. W., and Bemment, C. D. 2008. Nitrate attenuation in groundwater: a review of biogeochemical controlling processes. Water Resources Research 42:4215-4232.

Rücker, K. and Schrautzer, J., 2010. Nutrient retention function of a stream wetland complex—a high-frequency monitoring approach. Ecological Engineering 36:612-622.

Sapek, A., Sapek, B., Chrzanowski, S., and Jaszczymnski, J. 2007. Mobilization of substances in peat soils and their transfer within the groundwater and into surface water: Restoration of peatland soils for agricultural use. Agronomy Research (Tartu) 5:155–163.

Siegel, S. and Castellan, J., 1988. 26. Non parametric statistics for the behavioral sciences. New York: Graw-Hill p.213-214.

Sponseller, R. A., Blackburn, M., Nilsson, M. B., and Laudon, H. 2018. Headwater mires constitute a major source of nitrogen (N) to surface waters in the boreal landscape. Ecosystems 21:31-44.

Stanford, J. A., and Ward, J. V. 1993. An ecosystem perspective of alluvial rivers: connectivity and the hyporheic corridor. Journal of the North American Benthological Society. 12:48-60.

Tesoriero, A. J., Spruill, T. B., Mew Jr, H. E., Farrell, K. M., and Harden, S. L., 2005. Nitrogen transport and transformations in a coastal plain watershed: Influence of geomorphology on flow paths and residence times. Water Resources Research 41.

Thorp, J.H., Thoms, M.C. and Delong, M.D., 2006. The riverine ecosystem synthesis: biocomplexity in river networks across space and time. River Research and Applications 22:123-147.

Thorslund, J., Jarsjo, J., Jaramillo, F., Jawitz, J.W., Manzoni, S., Basu, N.B., Chalov, S.R., Cohen, M.J., Creed, I.F., Goldenberg, R. and Hylin, A., 2017. Wetlands as large-scale nature-based solutions: Status and challenges for research, engineering and management. Ecological Engineering 108:489-497.

Tiedje, J.M., 1988. Ecology of denitrification and dissimilatory nitrate reduction to ammonium. Biology of anaerobic microorganisms, 717:179-244.

Toth, J., 1963. A theoretical analysis of groundwater flow in small drainage basins. Journal of geophysical research, 68:4795-4812.

U.S. EPA. 1986. Method 9251: Chloride (colorimetric, automated Ferricyanide AAII).

U.S. EPA. 1993a. Method 350.1: Determination of ammonia N by semi-automated colorimetry. Environmental Monitoring Systems Laboratory. Office of Research and Development. Cincinnati OH.

U.S. EPA. 1993b. Method 353.1, Revision 2.0: Determination of nitrate-nitrite N by automated colorimetry. Environmental Monitoring Systems Laboratory. Office of Research and Development. Cincinnati OH.

U.S. EPA. 1993c. Method 365.1, Revision 2.0: Determination of phosphorus by semi-automated colorimetry. Environmental Monitoring Systems Laboratory. Office of Research and Development. Cincinnati OH.

U.S. EPA. 2005. Method 415.3: Measurement of total organic carbon, dissolved organic carbon, and specific UV absorbance at 254nm in source water and drinking water. Cincinnati, Ohio.

U.S. Geological Survey (USGS). 2020. National Water Information System.https://waterdata.usgs.gov/mt/nwis/uv?site_no=12323850

Vidon, P.G. and Hill, A.R. 2004. Landscape controls on nitrate removal in stream riparian zones. Water Resources Research, 40.

Vogel, R.M., Wilson, I. and Daly, C., 1999. Regional regression models of annual streamflow for the United States. Journal of Irrigation and Drainage Engineering 125:148-157.

Wanek, A.A. and Barclay, C.S., 1966. Geology of the northwest quarter of the Anaconda quadrangle, Deer Lodge County, Montana.

Wang, H., Richardson, C. J., Ho, M., and Flanagan, N. (2016). Drained coastal peatlands: A potential nitrogen source to marine ecosystems under prolonged drought and heavy storm events—A microcosm experiment. Science of the Total Environment 566:621–626.

Watanabe, A., Tsutsuki, K., Inoue, Y., Maie, N., Melling, L., and Jaffé, R., 2014. Composition of dissolved organic nitrogen in rivers associated with wetlands. Science of the total environment 493:220-228.

Water and Environmental Technologies, 2003. Anaconda Well Field Source Water Delineation and Assessment Report. PWSID# MT-0000016. 1485 Continental Drive Butte, MT 59701

Webster, J.R., Mulholland, P.J., Tank, J.L., Valett, H.M., Dodds, W.K., Peterson, B.J., Bowden, W.B., Dahm, C.N., Findlay, S., Gregory, S.V. and Grimm, N.B., 2003. Factors affecting ammonium uptake in streams–an inter-biome perspective. Freshwater Biology 48:1329-1352.

Wilson, J.L. and Guan, H., 2004. Mountain-block hydrology and mountain-front recharge. Groundwater recharge in a desert environment: The Southwestern United States. 9.

Winter, T. C. 1999. Relation of streams, lakes, and wetlands to groundwater flow systems. Hydrogeology Journal, 7:28-45.

Wong, L.S., R. Hashim and F.H. Ali, 2009. A Review on Hydraulic Conductivity and Compressibility of Peat. Journal of Applied Sciences 9:3207-3218.

871 Wroblicky, G. J., Campana, M. E., Valett, H. M., and Dahm, C. N. 1998. Seasonal variation in surface-
872 subsurface water exchange and lateral hyporheic area of two stream-aquifer systems. Water
873 Resources Research, 34:317-328.

874

875

876

877

878

879

880

881

882

883

884

885

886

887

888

889

890

891

892

893

894

895

896

897

898

899

900

901

902

Supplemental Information

Substrate Layer

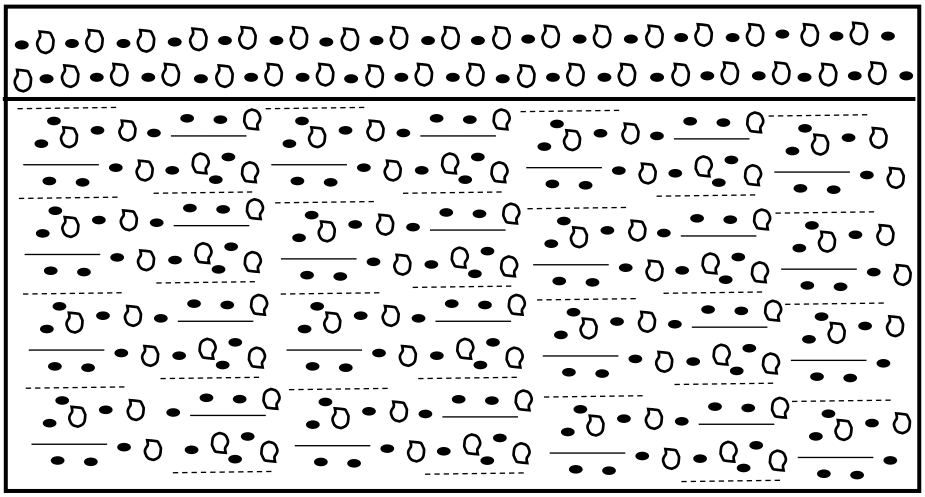

Figure S1: Schematic of the surficial aquifer's geologic substrate.

Table S1: Chloride concentrations of diffuse groundwater input (Cl_{dif}) into the four reaches of Lost Creek on various sampling days.

	Cl_{dif} (mg L^{-1})			
Date	Reach I	Reach II	Reach III	Reach IV
5/31/2020	8.97	10.10	-	-
7/1/2020	-	6.10	-	-
7/28/2020	6.67	6.27	-	-
8/27/2020	9.91	5.70	-	0.21
10/2/2020	7.12	8.41	17.46	10.77

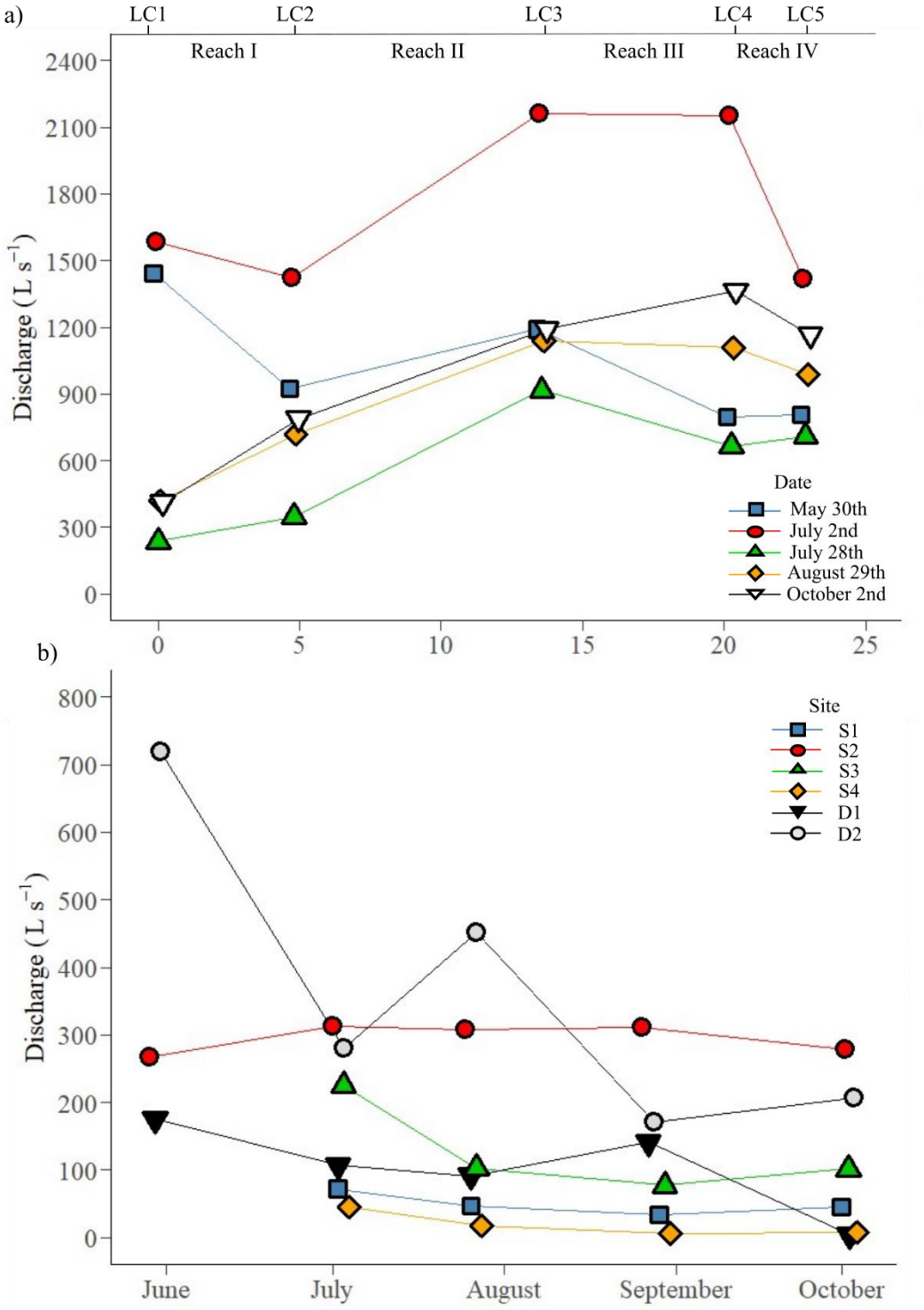

Figure S2: a) Stream flow measurements (Discharge, L s^{-1}) at five sites (LC1-5) that form the four reaches along Lost Creek. Reaches are delineated along the top of panel a. Points in panel a are colored by the sampling date and plotted against river distance from LC1. b) Discharge measurements at two irrigation diversions (D1-2, black squares and circles) and the four spring brooks (S1-S4).

960

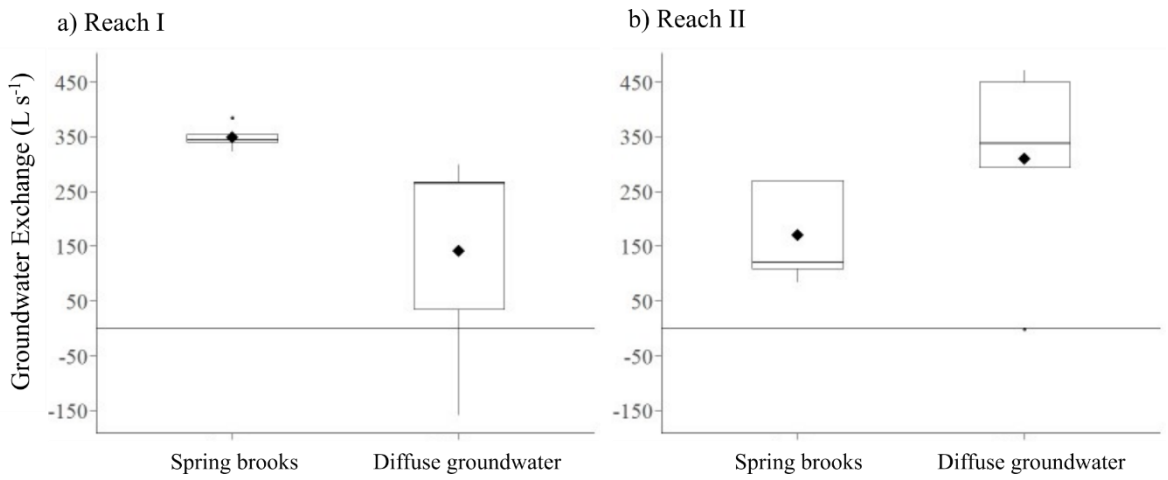

Figure S3: Magnitude and types of groundwater discharge to Lost Creek associated with spring brooks or diffuse groundwater exchange across all sampling dates for reaches I (a) and II (b). Boxplots include the 25th and 75th percentiles (box limits), median (central line), values in the lowest and highest quartiles (whiskers), significant outliers (exceeding the absolute value of the 25th or 75th quartiles minus 1.5-times the interquartile range), and the mean (black diamond).

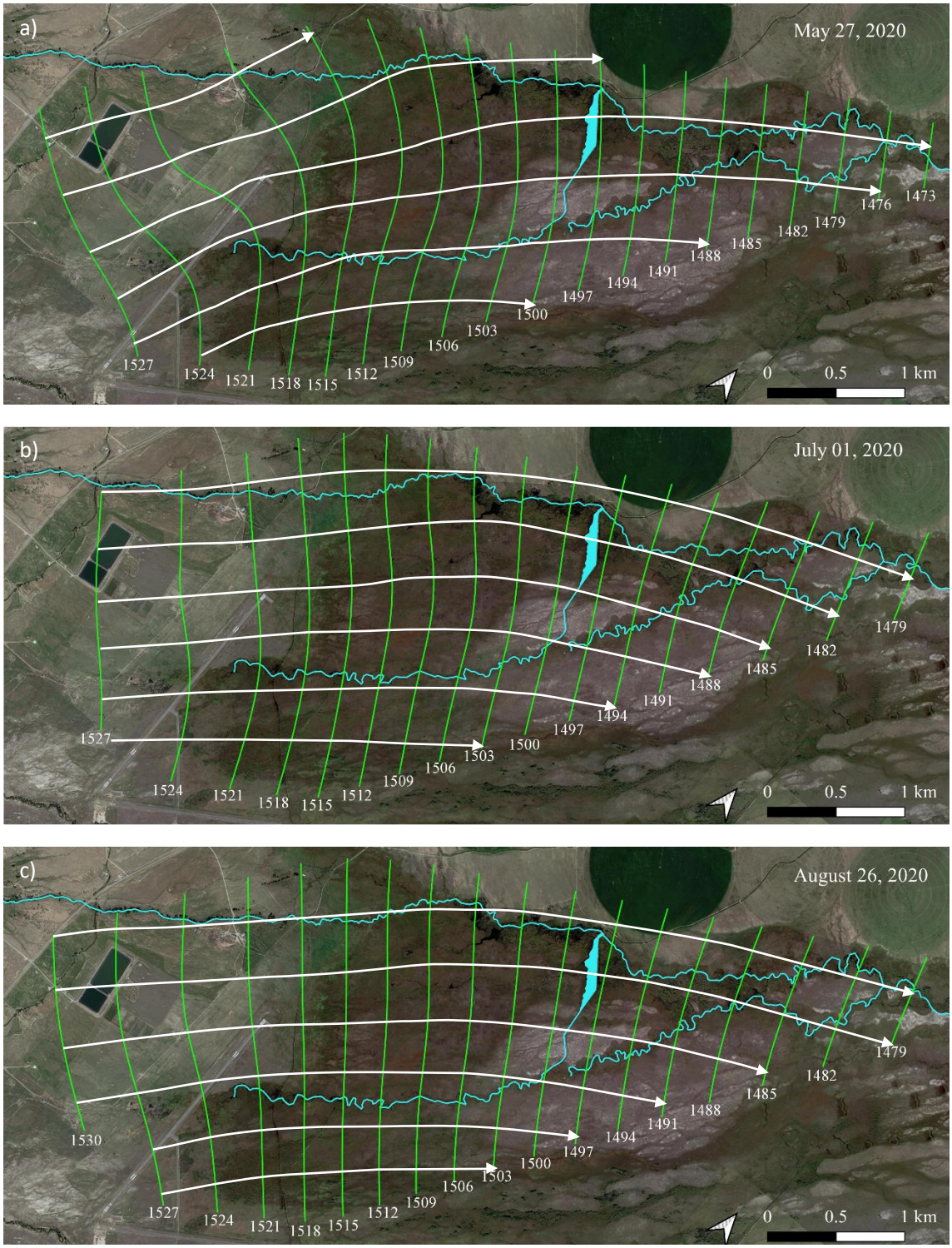

Figure S4: Aerial image of the LCDC with water table elevations (green equipotential contours, meters above sea level) and flownet (white streamlines) during May (a), July (b), and August (c) of 2020. Groundwater moves from high to low elevation crossing equipotential contours at right angles.

977

978

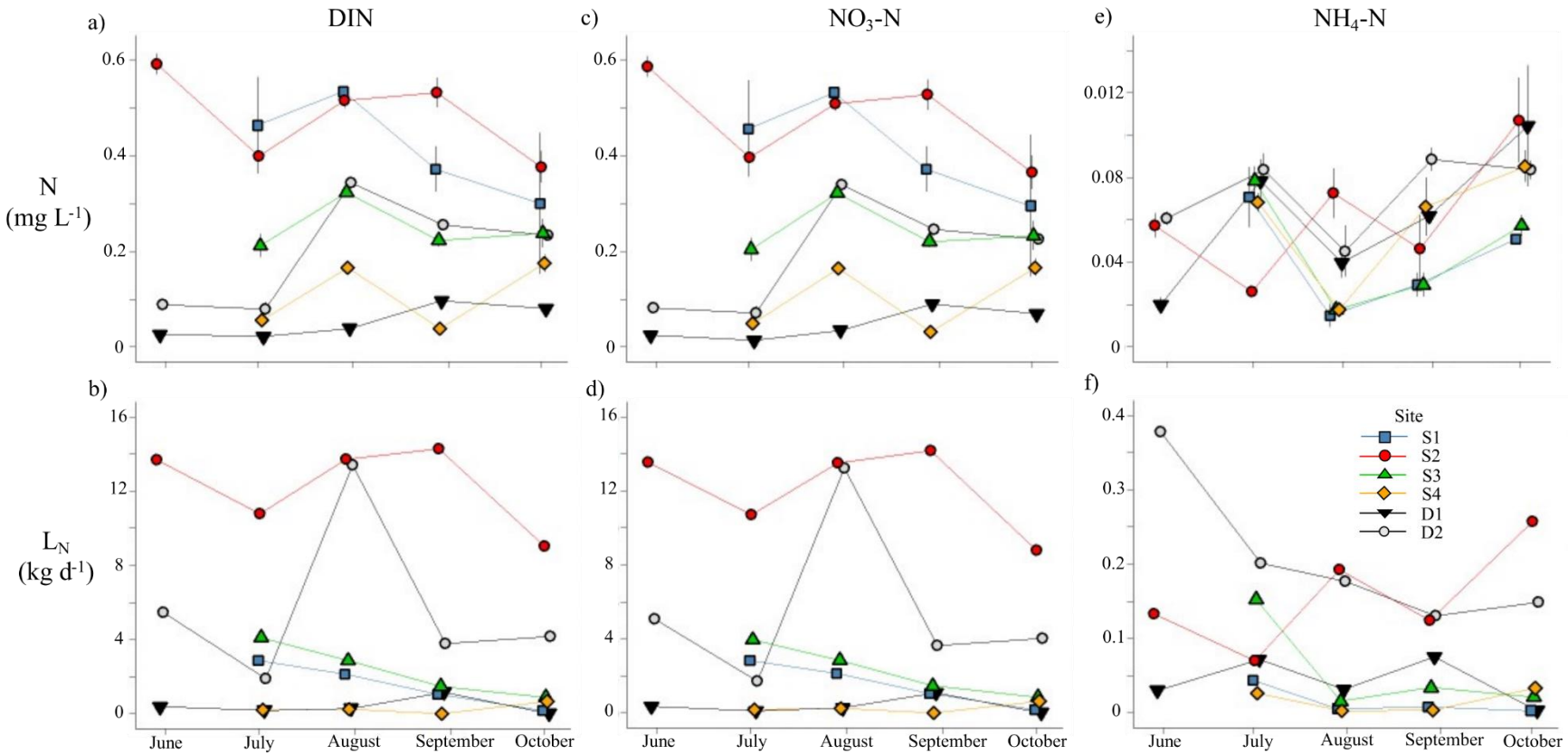

Figure S5: Concentrations of DIN (a) and individual N species (c, e) and their respective loads (b, d, f) at two irrigation diversions (D1-2) and four spring brooks (S1-S4). Points are colored by the sampling site and plotted by the sampling date. Data are means ± standard error.

979

980

981

982

983

984

Table S2: Effective biogeochemical flux (U_{bio}) for NH_4-N, NO_3-N and DIN in reaches I-IV across the five sampling dates.

Date	NH_4-N (mg m^{-2} d^{-1})	NO_3-N (mg m^{-2} d^{-1})	DIN (mg m^{-2} d^{-1})
Reach I			
5/31/2020	-29.95	71.02	41.23
7/1/2020	-12.32	259.7	246.85
7/28/2020	-225.37	325.61	101.55
8/27/2020	-189.25	185.79	-2.29
10/2/2020	-219.59	236.82	18.54
Reach II			
5/31/2020	-3.83	158.67	154.85
7/1/2020	-174.2	-37.77	-210.98
7/28/2020	-155.83	183.97	29.1
8/27/2020	-122.05	71.27	-50.07
10/2/2020	-110.35	247.18	137.49
Reach III			
5/31/2020	9.34	-70.7	-61.37
7/1/2020	16.67	-348.65	-327.81
7/28/2020	24.25	-283.72	-258.79
8/27/2020	162.79	-228.81	-66.02
10/2/2020	-57.6	136.79	79.66
Reach IV			
5/31/2020	-25.98	-237.28	-245.58
7/1/2020	-28.03	-636.53	-668.46
7/28/2020	-135.16	180.85	46.11
8/27/2020	-55.86	-43.54	-99.4
10/2/2020	-34.41	-1054.2	-1088.62

985

986

987

988

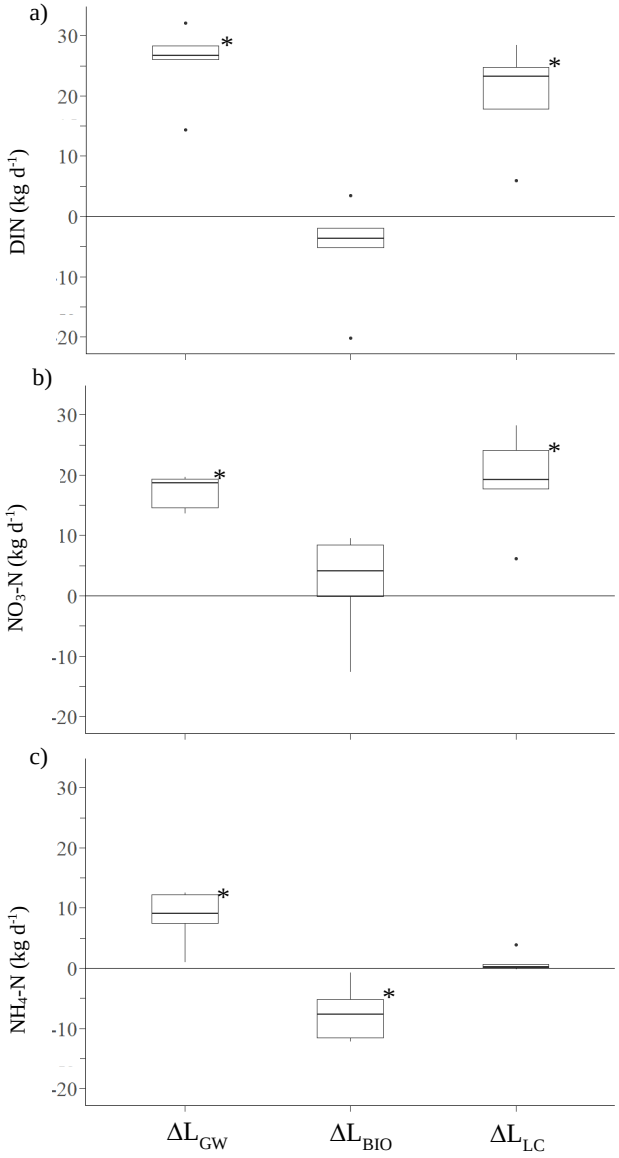

Figure S6: Lost Creek scale changes in load (ΔL_{LC}) partitioned into net groundwater exchange (ΔL_{GW}) and net biogeochemical processing (ΔL_{BIO}) for DIN (a), NO_3-N (b), and NH_4-N (c) on all sampling dates. Boxplots include the 25th and 75th percentiles (box limits), median (central line), values in the lowest and highest quartiles (whiskers), and significant outliers (exceeding the absolute value of the 25th or 75th quartiles minus 1.5-times the interquartile range). Asterisks indicate mean values are significantly different ($p < 0.05$) from zero following one-sample location t-tests.

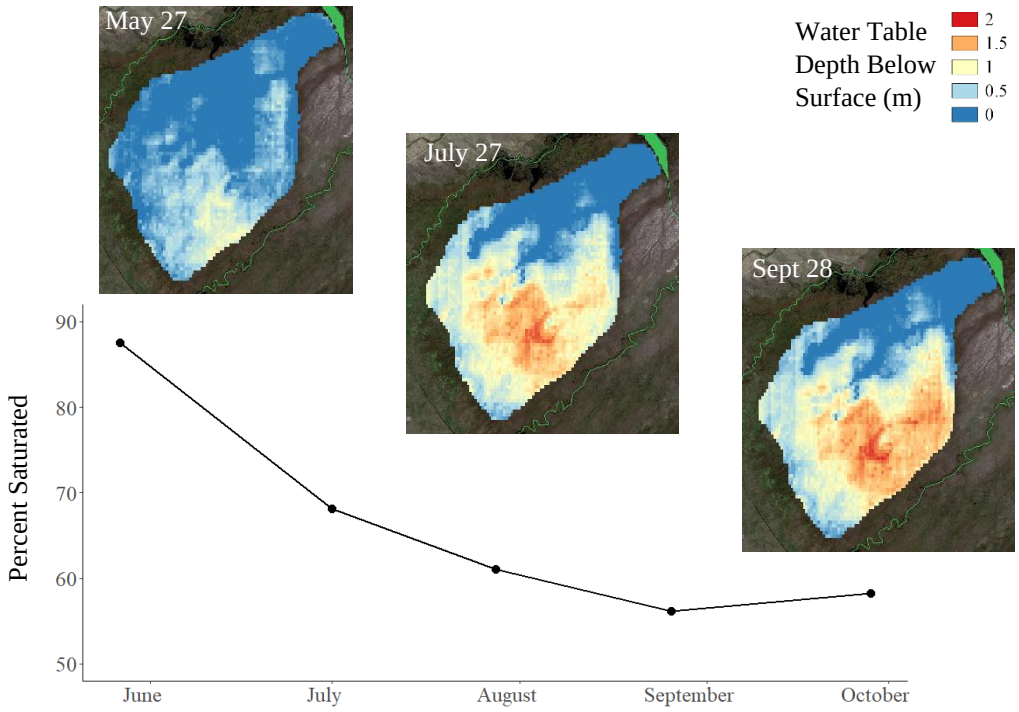

Figure S7: Progression of fen saturation with associated aerial raster images depicting temporal and spatial variability of the depth of unsaturated wetland material.